PHILOSOPHICAL TRANSACTIONS OF THE ROYAL SOCIETY A MATHEMATICAL, PHYSICAL & ENGINEERING SCIENCES

The Statistical Properties of Echoes Diffracted from Rough Surfaces

M. V. Berry

Phil. Trans. R. Soc. Lond. A 1973 **273**, 611-654
doi: 10.1098/rsta.1973.0019

THE STATISTICAL PROPERTIES OF ECHOES DIFFRACTED FROM ROUGH SURFACES

By M. V. BERRY

H. H. Wills Physics Laboratory, Tyndall Avenue, Bristol BS8 1TL

(*Communicated by J. M. Ziman, F.R.S. – Received 22 August* 1972)

CONTENTS

This work aims to provide the statistical theory behind recent wide-angle pulsed radar experiments to determine the topography and roughness of (*a*) polar glacier beds from measurements near the snow surface, and (*b*) the lunar surface from satellites in close orbit. We analyse the statistical properties of the echo received back at the source when a quasimonochromatic pulse of radiation, isotropic in direction, is reflected from a rough surface which is a random perturbation of a horizontal plane. Kirchhoff diffraction theory is employed, so that multiple scattering and shadowing are neglected. But the r.m.s. surface height is unrestricted, and closed formulae are obtained which are valid through the transition from coherence (flat-mirror surface) to incoherence (surface of high relief, to which geometrical optics is applicable).

Vol. 273. A. 1237. (Price £1.15; U.S. $3.20) 49 [Published 15 February 1973

For fixed source-receiver height the average echo wavefunction, and the average echo power, are calculated as functions of delay time, and the echo autocorrelation function is calculated as a function of the separation of two source-receiver points at fixed delay time. The duration of the echo is calculated, and the long-wave limit, the smooth-surface limit, the Fraunhofer limit, the continuous wave limit and the geometrical-optics limit are examined. A method is suggested for inferring the statistics of the surface from measurements of the average echo power. The theory of random noise is applied to the fluctuations about the calculated averages which occur as the source-receiver is moved horizontally. These fluctuations constitute 'spatial fading', and we calculate several measures of the spatial fading rate for the echo wavefunction and the time-smoothed echo power, as well as a measure of the degree of spatial periodicity of the fading. Finally, an estimate is made of the smallest detectable horizontal displacement of the source-receiver relative to the rough surface.

List of principal symbols

Symbol,	*meaning and equation, etc., where introduced*
$a(t)$	pulse envelope function (2.2)
$\bar{a}(\omega)$	(2.3)
c	speed of waves
$C_f(\boldsymbol{R})$	autocorrelation function of surface height (3.11)
$C_Z(\boldsymbol{R})$	autocorrelation function of surface reflectivity (3.31)
$C_\rho(\boldsymbol{R})$	autocorrelation function of echo amplitude (4.28)
$C_{\rho 2}(\boldsymbol{R})$	autocorrelation function of smoothed echo power (4.22)
$C_\xi(\boldsymbol{R}), C_\psi(\tau, \boldsymbol{R})$	autocorrelation function of echo wavefunction (4.1)
$C_{\psi_c \psi_c^*}(\boldsymbol{R})$	autocorrelation function of complex echo wavefunction (4.20)
E	total energy in the echo (6.4)
$E(\boldsymbol{K}, \tau)$	'spatial power spectrum' of echo (7.20)
$\mathscr{E}(q, \tau)$	'modified spatial power spectrum' of echo (7.24)
$f(\boldsymbol{R})$	height of rough surface above point $\boldsymbol{R}$ on the reference plane
f'	surface slope (3.15)
$F(t)$	time dependence of pulse (2.1)
$F_c(t)$	time dependence of complex pulse (2.3)
$\bar{F}(\omega)$	Fourier transform of $F(t)$ (2.2)
h	height of source-receiver above reference plane
$\boldsymbol{K}$	wave vector of plane wave component of echo (7.20)
L	horizontal extent of typical surface irregularity
n	spatial rate of change of ρ at a particular place ÷ r.m.s. rate of change of ρ (7.40)
N_f	linear density of surface zero-crossings (3.14)
$N_\xi(\langle\xi\rangle), N_\xi(\tau)$	linear density of crossings of mean level by wavefunction (4.9), (7.1)
$N_\rho(\rho_D), N_\rho^{\max}(\tau)$	linear density of crossings of a given amplitude level (4.36), (4.40)
$P_1^f(f)$	one-position surface probability distribution (3.1)
$\bar{P}_1^f(k)$	(3.3)
$P_2^f(f_1, f_2, \boldsymbol{R}_2 - \boldsymbol{R}_1)$	two-position surface probability distribution (3.6)
$\bar{P}_2^f(k_1, k_2, \boldsymbol{R})$	(3.8)
$P_2^\xi(\xi_1, \xi_2, \boldsymbol{R})$	two-position echo probability distribution (4.4)
$P_2^\rho(\rho_1, \rho_2, \boldsymbol{R})$	two-position amplitude probability distribution (4.24)
q	wave-number of plane wave component of echo (7.24)
$Q(\tau)$	(5.35), (5.36)
$Q(\omega_1, \omega_2, \tau)$	(5.15), (5.16)
$Q_Z(\tau)$	(5.31), (5.32)

r	distance from source
$\boldsymbol{R}$	two-dimensional position vector in reference plane, separation of two source-receiver positions
$\boldsymbol{R}_0$	horizontal position vector of source-receiver
$R(\tau)$	radius of annulus on surface returning radiation at τ (2.15)
$R_{\max}(\tau)$	source-receiver separation beyond which no spatial correlation exists between echoes (7.32)
S	r.m.s. surface height above reference plane
t	time measured from emission of pulse centre from source
T	echo half-length (§6 (iii))
T_Σ	half-length of echo variance (§6 (iii))
T_s	smoothing time (§2 (ii))
$Z, Z(\boldsymbol{R})$	amplitude reflectivity of rough surface at $\boldsymbol{R}$
α	undulating surface (§3 (i))
β	surface of steps (§3 (ii))
γ	flat surface of varying reflectivity (§3 (iii))
δ	coherence parameter (5.33), (5.34)
$\Delta R(\tau)$	width of annulus on surface returning radiation at τ (2.16)
$\lvert\Delta \boldsymbol{R}_0\rvert_{\min}$	smallest detectable horizontal displacement of source-receiver (7.43)
$\lvert\Delta \boldsymbol{R}_0\rvert_0$	mean distance between zeros of echo wavefunction (7.14)
$\Delta\theta(\tau)$	(2.18), figure 2
$\Delta\rho$	smallest detectable change in echo amplitude level (§7 (ii))
$\Delta\omega$	pulse band width (2.22)
$\epsilon(\tau)$	parameter specifying spectral purity of spatial fading (7.19)
η	imaginary part of complex echo wavefunction (4.3)
$\theta(\tau)$	semi-angle of cone returning radiation at τ (2.17)
$\theta_{\max}$	semi-angle of cone containing most of the radiation returned to the source (§2 (i))
λ	carrier wavelength of pulse
ξ	echo wave function (4.3)
$\Pi(f')$	probability distribution of surface slopes (3.15)
$\Pi(\rho, \rho')$	joint probability distribution of ρ and spatial rate of change of ρ (4.34)
ρ	echo amplitude (4.3)
σ	spatial pulse length
$\Sigma, \Sigma_\xi, \Sigma(\tau)$	echo variance (4.7), (4.18a)
τ	delay time (2.11)
τ'	dummy delay time variable (5.13 ff.) labelling rings within the contributing annulus of figure 2
$\bar{\tau}(\tau)$	modified delay time (7.2), (7.3) figure 6
$\phi(r, t)$	outgoing wave from source (2.1)
χ	phase of complex echo wavefunction (4.3)
$\psi(\tau, \boldsymbol{R}_0)$	echo wavefunction (§2 (i))
$\psi_c(\tau, \boldsymbol{R}_0)$	complex echo wavefunction (§2 (ii))
$\bar{\psi}(\omega, \boldsymbol{R}_0)$	§2 (ii)
ω_0	carrier angular frequency of pulse

1. Introduction

It is very difficult to calculate all the details of the echo received back at the source when a pulse of radiation is reflected from a rough surface; it is even more difficult, in principle as well as in practice, to infer the detailed topography of the surface from measurements on the echo (Berry 1972). Fortunately, the interpretation of the data obtained by practical methods of echo sounding does not generally require these two problems to be solved completely. Consider, for example, the pulsed radar experiments described by Robin, Evans & Bailey (1969), whose aim is to ascertain the subglacial topography of polar regions. In order to determine the gross features of the ice/rock interface – the 'geography' – it is necessary merely to note how the time of the 'first return' of the echo varies as the source-receiver point is moved in a plane above the surface.† Of course, the fine detail in the interface – its 'roughness' – also affects the echo, which may differ considerably from the original pulse both in its duration and its detailed structure. A detailed knowledge of the roughness and of the echo is not usually required, however; *statistical* information is sufficient. For instance, instead of seeking the location and dimensions of every boulder near the rock surface, we may be content to know approximately how many boulders in a given size range lie on unit area of the surface. Or, instead of asking precisely how the echo strength at a given delay time will 'fade' when the source-receiver is moved from one particular point above the surface to another, we may wish to know only the *average* rate of change of the echo strength (this is what determines the ultimate sensitivity of the technique of ice velocity measurement proposed by Nye, Kyte & Threlfall (1972*a*) and pioneered by Walford (1972)).

In this paper we set up a framework within which such statistical questions can be answered. We introduce an ensemble of statistically stationary surfaces whose roughness resembles that of the actual rough surface, and use this ensemble to calculate the average values of a variety of quantities associated with the echo. We believe these averages to correspond to 'local averages' computed from measurements of the echo for a large number of source-receiver positions, all of which lie above a given 'neighbourhood' of the actual rough surface. This is necessary, because otherwise we would be averaging not only over the 'roughness' but also over the mountains and valleys corresponding to 'geography'. But it will be the exception, rather than the rule, that roughness and geography can be clearly separated, because naturally occurring surfaces may vary on all scales (Nye 1970, p. 385), and care must be taken in defining the size of the neighbourhoods involved in the averaging. A proper theory of this 'partial averaging' is not available, but it is clear that the neighbourhoods must be at least as large as the area of the surface which is explored by the pulse from a single source-receiver position P; this is the surface lying within a cone with apex P, whose axis is perpendicular to the mean surface and whose semi-angle is typically about 10° (see § 6 (iii)). (Most of the previous work on reflexion from rough surfaces has been concerned with incident plane waves of infinite extent (Beckmann & Spizzichino 1963), or with statistically homogeneous surfaces (Booker, Ratcliffe & Shinn 1950), so that this problem of neighbourhoods has not arisen.)

The rough surface is specified by its height $f(\boldsymbol{R})$ (figure 1) above a 'reference plane', which we shall refer to as 'horizontal'. It is convenient to define this plane as the mean surface over the neighbourhood explored by the experiment; the two-dimensional vector $\boldsymbol{R}$ locates a point in the plane. The scale of the roughness is characterized by the local r.m.s. surface height S and

† The 'deconvolution' of these first returns is not quite straightforward (Harrison 1970; J. F. Nye unpublished; Ozorio unpublished), particularly if there is a series of reflecting layers within the ice.

the horizontal extent L of a typical irregularity. The source-receiver P (whose polar diagram is assumed isotropic) is at a height h vertically above the position $\boldsymbol{R}_0$ on the reference plane. The pulse sent out from P is specified by its time-dependence $F(t)$ (defined in §2 (i)), and travels to and from the surface with the constant speed c (in the polar experiments of Robin *et al.* (1969), c is the speed of radar waves in glacier ice). It is common for echo-sounding experiments to employ quasimonochromatic pulses, which are characterized by a carrier wavelength λ and a spatial pulse-length σ; thus $F(t)$ has a duration σ/c, and a predominant angular frequency ω_0 given by $2\pi c/\lambda$.

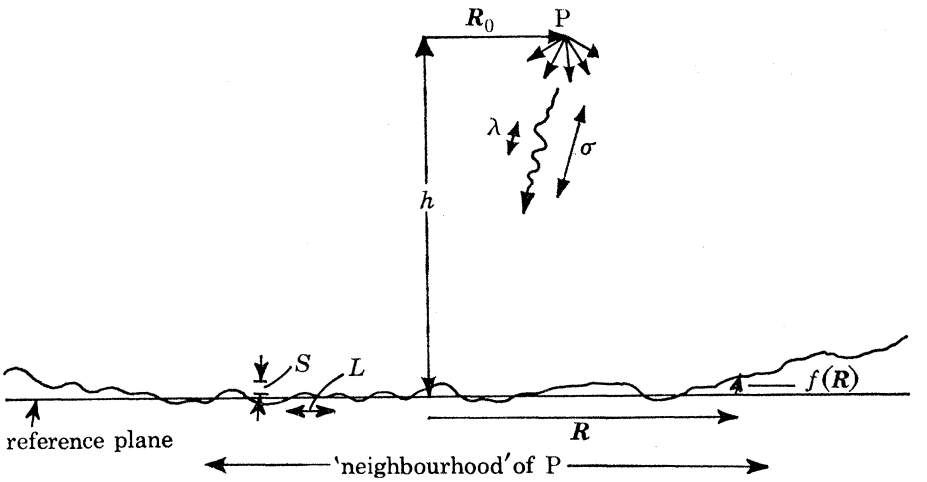

FIGURE 1. Basic geometry of system, and schematic definition of important length parameters.

We shall analyse the dependence of the various properties of the echo received back at P on the five length parameters h, λ, σ, S and L. The relative influence of these parameters is different in different parts of the echo, i.e. for different values of the time delay τ (defined in §2 (i)). In addition, two qualitatively different types of rough surface with the same values of S and L (described in §3) may give rise to very different echoes (§6). The irregular 'fading' of the echo as $\boldsymbol{R}_0$ is varied depends in principle on all five parameters, but we shall find in §7 that some aspects of this fading (e.g. the average fading wavelength) are surprisingly independent of S and L (i.e. of the form of the surface).

In our treatment the five parameters will be arbitrary, apart from the following four restrictions:

(*a*) Because of the quasi-monochromatic nature of the pulse, we require

$$\lambda \ll \sigma \tag{1.1}$$

(in Antarctic echo-sounding, $\lambda/\sigma \approx 0.1$).

(*b*) Kirchhoff diffraction theory will be employed throughout (see §2 (i) and Berry 1972); this neglects shadowing of one part of the surface by another (as seen from P), which will be a reasonable approximation if

$$S < L. \tag{1.2}$$

This is the most severe of the four restrictions; if it is violated, we are dealing either with a 'bed-of nails' surface or a surface covered with potholes.

(*c*) For Kirchhoff theory to be valid, P must not lie in the 'near zone' of the surface, i.e.

$$\lambda \ll h \tag{1.3}$$

(in Antarctic echo-sounding, λ/h is typically about 0.005).

(*d*) Considerable simplification in the mathematics (§2(i)) is produced by requiring that

$$S \ll h. \tag{1.4}$$

Violation of this condition might be produced by a high cliff in the 'neighbourhood' of P, which would be described as 'geography' rather than 'roughness'; the effects of any small-scale roughness near such a cliff cannot be described by the methods of this paper.

These restrictions (which are often satisfied in practical echo-sounding) leave a great deal of freedom in the possible values of h, λ, σ, S and L, corresponding to a great variety of echo behaviour (see, for example, §§6(ii)–6(viii)). Perhaps the most important of these 'degrees of freedom' is the fact that σ may be finite, although restricted by (1.1); thus we shall be able to describe fading in the 'tail' of the echo, which depends essentially *both* on the pulse being of finite duration *and* on the interference behaviour resulting from quasi-monochromaticity (§7(i)).

The paper is arranged as follows: In §2(i) the wave theory underlying our treatment is presented; this is a simple modification of Kirchhoff's theory, which we call the 'Fresnel approximation'. It is a common experimental practice to record not the echo wavefunction but the power, or the rectified wavefunction, smoothed over at least one carrier wave period; the analytical description of this smoothing is dealt with in §2(ii). In §3 the statistics of rough surfaces are introduced, and probability distributions, correlation functions, etc., are defined for three different types of surface. In §4 the important concept of *coherence* of the echo is introduced, and the statistical distributions associated with the echo are discussed. It is shown that under most circumstances the theory of Gaussian noise may be applied; this means that in order to describe the echo statistics completely it is necessary to calculate only: (i) the average echo wavefunction, (ii) the average echo power (i.e. square of wavefunction), and (iii) the autocorrelation function of the echo wavefunction at a given time delay τ as a function of the separation $\boldsymbol{R}$ of two source-receiver points. These three ensemble averages are calculated in §5 for the three types of rough surface introduced in §3. The formulae for the mean echo power are examined in detail in §6, in order to calculate the duration of the echo, and to describe the nature of the echo in a number of important limiting cases. We also (§6(ix)) suggest a systematic way of inferring the nature of the surface from the average power. In §7 the statistics of the pattern of spatial fading observed when the source-receiver position R_0 varies is examined with the aid of the echo autocorrelation function calculated in §5. The quasi-periodicity of the fading, whose 'wavelength' and spectral purity depend on the delay time τ, is discussed in §7(i), and in §7(ii) these results and the results of §6 are combined to yield a criterion for the ultimate sensitivity likely to be obtained by techniques which employ the spatial fading pattern for precise position location (Walford 1972).

It is hoped that a number of the formulae derived in this paper will prove useful to workers engaged in practical echo-sounding. In order to assist readers who have no interest in wading through the considerable analytical detail involved in deriving these formulae, they are gathered together at the beginning of §8.

There is an enormous literature on scattering from rough surfaces (see the treatise and bibliography by Beckmann & Spizzichino 1963). Our reason for adding to it is that a comprehensive theory for the diffraction of a *pulse* does not seem to have been published; most previous work is

confined to monochromatic waves, and can never explain the time-dependence and spatia fading of the echo tail (i.e. the late returns, for which $\tau > \sigma/2c$). In addition, conventional radar systems do not employ the very wide-angle (essentially isotropic) beams considered by us, which are used in the glaciological experiments of Robin *et al.* (1969), for which a laboratory simulation has been constructed (Nye *et al.* 1972*a*) involving ultrasonic pulses reflected from metal foil, and for which extensive computer simulations as well as a theory based on 'filter functions' have been devised by Harrison (1972). Inevitably, many of our results will have appeared before in various guises (particularly in the monumental works on random noise by Rice (1944, 1945), and the analysis of random surfaces (e.g. sea waves) by Longuet-Higgins (1956)); we consider that this repetition is worthwhile in the interests of clarity.

2. Diffraction theory

Neglecting polarization effects, we write the scalar wavefunction of the pulse emitted by the source as

$$\phi(r,t) \equiv \frac{F(t-(r/c))}{r}, \tag{2.1}$$

where r represents distance from the source-receiver, which is assumed to radiate and receive isotropically (this is not true in practice, but we shall presently see that this is not likely to give rise to serious error); the wavefunction is defined to make ϕ^2 have the dimensions of *power*. The time-dependence of the source is specified by the quasi-monochromatic function $F(t)$. We write this in the alternative forms

$$F(t) \equiv a(t)\cos\omega_0 t \equiv \int_{-\infty}^{\infty} \mathrm{d}\omega\, \bar{F}(\omega)\exp\{-\mathrm{i}\omega t\} \equiv \mathrm{Re}\, F_c(t), \tag{2.2}$$

where $a(t)$ is the pulse envelope of approximate duration σ/c, ω_0 is the angular frequency of the carrier wave, a bar above a function denotes Fourier transformation with respect to the argument, and $F_c(t)$ is a complex source function, defined by

$$F_c(t) \equiv a(t)\exp\{-\mathrm{i}\omega_0 t\} \equiv \int_{-\infty}^{\infty} \mathrm{d}\omega\, \bar{a}(\omega-\omega_0)\exp\{-\mathrm{i}\omega_0 t\}. \tag{2.3}$$

As a simple model useful for analytical purposes, we may take the Gaussian pulse envelope

$$a(t) = A\exp\{-c^2t^2/\sigma^2\}, \tag{2.4}$$

where σ/c is twice the r.m.s. pulse duration for the power envelope, defined by

$$\sigma = 2c\left(\int_{-\infty}^{\infty} \mathrm{d}t\, t^2a^2(t) \Big/ \int_{-\infty}^{\infty} \mathrm{d}t\, a^2(t)\right)^{\frac{1}{2}}. \tag{2.5}$$

2 (i). *The Fresnel approximation*

According to Kirchhoff diffraction theory, the echo wavefunction $\psi(t, \boldsymbol{R}_0)$ received back at the source at $\boldsymbol{R}_0$ at time t is given by an integral over the rough surface, each point of which acts as a 'secondary source' for the reflexion of the incident wave $\phi(r,t)$.

It was shown by Berry (1972) that this integral may be transformed into an integral over points $\boldsymbol{R}$ in the reference plane (figure 1). When we introduce a position-dependent amplitude

reflectivity $Z(\boldsymbol{R})$ to allow for the fact that the surface may not be a perfect mirror (which would correspond to $Z = 1$), the expression for the echo wavefunction is

$$\psi(t, \boldsymbol{R}_0) = -\frac{1}{2\pi c}\iint \mathrm{d}\boldsymbol{R}\, \frac{Z(\boldsymbol{R})\, F'[t-(2/c)\sqrt{\{(h-f(\boldsymbol{R}))^2+(\boldsymbol{R}-\boldsymbol{R}_0)^2\}}]}{(h-f(\boldsymbol{R}))\sqrt{\{(h-f(\boldsymbol{R}))^2+(\boldsymbol{R}-\boldsymbol{R}_0)^2\}}}. \tag{2.6}$$

The prime denotes differentiation of F by its argument.

Because of the way $f(\boldsymbol{R})$ appears in this formula, it is intractable for the purpose of taking ensemble averages. In this paper we shall adopt a simplification of (2.6) – the 'Fresnel approximation' – which consists in writing the square root in the numerator as

$$\sqrt{\{(h-f(\boldsymbol{R}))^2+(\boldsymbol{R}-\boldsymbol{R}_0)^2\}} \approx h-f(\boldsymbol{R})+(\boldsymbol{R}-\boldsymbol{R}_0)^2/2h, \tag{2.7}$$

and replacing the denominator in the integrand by h^2. There are really two assumptions here; first, we are requiring that

$$f(\boldsymbol{R}) \ll h \tag{2.8}$$

for all surface points $\boldsymbol{R}$ which contribute significantly to the integral. This is equivalent to the approximation (1.4) already discussed. The second and principal assumption underlying (2.7) is a restriction on the semi-angle $\theta_{\max}$ of the cone within which radiation is returned to the source P (figure 2). The angle θ corresponding to a given point $\boldsymbol{R}$ on the surface is defined by

$$\tan\theta \equiv |\boldsymbol{R}-\boldsymbol{R}_0|/h. \tag{2.9}$$

By simply expanding the square root, it is easily seen that the approximation (2.7) is valid if

$$(\tan\theta_{\max})^4 \ll 8, \tag{2.10}$$

i.e. provided $\theta_{\max}$ does not exceed about 45°. This is not a severe restriction in practice, because the cones of illuminating radiation from radar aerials, etc., are often not much wider than this. Even from a theoretical standpoint there will often be no objection to using (2.7); first, because it is not expected that radiation will normally come back from large angles, as we shall see in §6(iii), and secondly, because the whole Kirchhoff approach must break down at very large angles owing to the inevitable shadowing which will then occur for all except perfectly flat surfaces. It is natural to measure time delay in the echo not from the instant $t = 0$ when the centre of the original pulse is emitted (cf. (2.4)), but from the instant $t = 2h/c$ when the centre of the pulse would be received at P after reflexion from the reference plane. Therefore we define the echo time delay

$$\tau \equiv t-2h/c. \tag{2.11}$$

If (2.7) and (2.11) are incorporated into (2.6), we obtain the Fresnel approximation for the echo wavefunction $\psi(\tau, \boldsymbol{R}_0)$:

$$\psi(\tau, \boldsymbol{R}_0) = -\frac{1}{2\pi ch^2}\iint \mathrm{d}\boldsymbol{R}\, Z(\boldsymbol{R})\, F'\left(\tau+\frac{2f(\boldsymbol{R})}{c}-\frac{(\boldsymbol{R}-\boldsymbol{R}_0)^2}{ch}\right). \tag{2.12}$$

A simple test of this expression can be carried out for a flat mirror surface ($f = 0, Z = 1$); evaluating the integral gives

$$\psi(\tau, \boldsymbol{R}_0) = -F(\tau)/2h, \tag{2.13}$$

which is precisely the result expected, describing the reflexion (with sign reversal) of the wave (2.1) from an image $2h$ below P.

The conditions (1.1 to 1.4) do not imply that

$$\sigma \ll h. \tag{2.14}$$

This restriction was not made, because we wish to be able to take the monochromatic limit $\sigma \to \infty$, which corresponds to continuous-wave illumination of the surface. Nevertheless, (2.14) is often satisfied in practical echo-sounding, and it is easy to see that in this case the radiation received at delay time τ has come mainly from an annulus on the surface (figure 2) which is exactly circular in view of (2.8). The radius $R(\tau)$ of this annulus and its width $\Delta R(\tau)$ are given by

$$R(\tau) = (ch\tau + \tfrac{1}{4}c^2\tau^2)^{\frac{1}{2}} \xrightarrow{\tau \to 0} (ch\tau)^{\frac{1}{2}} \tag{2.15}$$

and

$$\Delta R(\tau) = \frac{(h + \frac{1}{2}c\tau)\,\sigma}{2R(\tau)} \xrightarrow{\tau \to 0} \frac{\sigma}{2}\left(\frac{h}{c\tau}\right)^{\frac{1}{2}}. \tag{2.16}$$

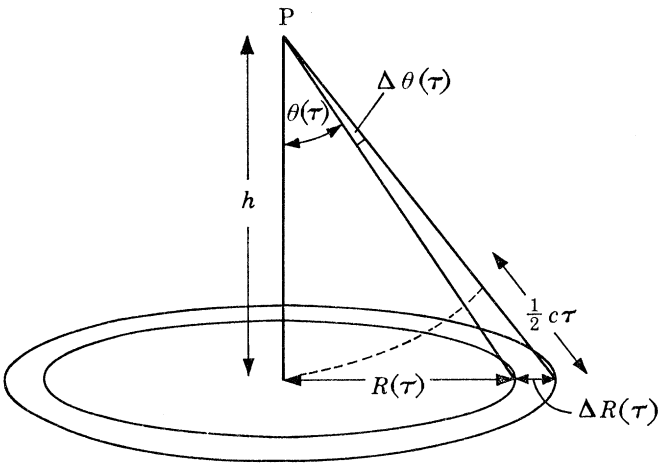

FIGURE 2. Annulus and cone of illuminating radiation contributing to echo received at time delay τ.

The annulus is contained within two cones whose semi-angles are $\theta(\tau)$ and $\theta(\tau) + \Delta\theta(\tau)$, where

$$\tau = \frac{4h}{c}\frac{\sin^2(\frac{1}{2}\theta(\tau))}{\cos\theta(\tau)} \xrightarrow{\tau \to 0} \frac{h\theta^2(\tau)}{c} \tag{2.17}$$

and

$$\Delta\theta(\tau) = \frac{\sigma\cos^2\theta(\tau)}{2h\sin\theta(\tau)} \xrightarrow{\tau \to 0} \frac{\sigma}{2(hc\tau)^{\frac{1}{2}}}. \tag{2.18}$$

The limiting values in (2.15) to (2.18) provide good approximations if θ does not exceed $\theta_{\max}$ given by (2.10).

It should not be supposed that the circles in figure 2 correspond to 'Fresnel zones' on the surface; these are generally highly convoluted (and possibly multiply-connected) lines lying mostly within the annulus (see Berry 1972). The detailed structure of particular Fresnel zones does not affect the statistical quantities with which this work is concerned.

2 (ii). *Smoothing the echo power*

The echo $\psi(\tau, \boldsymbol{R}_0)$ is a quasimonochromatic function of τ; this follows from the basic diffraction formula (2.12), given the nature of the original pulse $F(t)$ (equation (2.2)). It is a common experimental practice to eliminate the carrier-frequency oscillations by electronically smoothing the echo power $\psi^2(\tau, \boldsymbol{R}_0)$ over a time T_s comparable with the carrier-wave period

$$\lambda/c\,(= 2\pi/\omega_0).$$

We shall show that the smoothed echo power $(\psi^2(\tau, \boldsymbol{R}_0)_{\rm sm}$ is given to a very close approximation by

$$(\psi^2(\tau, \boldsymbol{R}_0))_{\rm sm} = \tfrac{1}{2}|\psi_{\rm c}(\tau, \boldsymbol{R}_0)|^2, \tag{2.19}$$

where $\psi_{\rm c}(\tau, \boldsymbol{R}_0)$ is the complex echo wavefunction resulting from the diffraction of the complex source function $F_{\rm c}(t)$, defined by (2.3).

It is convenient to employ Gaussian smoothing, so that

$$(\psi^2(\tau, \boldsymbol{R}_0))_{\rm sm} \equiv \frac{1}{(2\pi)^{\frac{1}{2}}T_{\rm s}}\int_{-\infty}^{\infty} {\rm d}\tau' \psi^2(\tau', \boldsymbol{R}_0) \exp\{-(\tau-\tau')^2/2T_{\rm s}^2\}, \tag{2.20}$$

$$= \int_{-\infty}^{\infty} {\rm d}\omega_1 \int_{-\infty}^{\infty} {\rm d}\omega_2 \, \overline{\psi}(\omega_1, \boldsymbol{R}_0)\, \overline{\psi}(\omega_2, \boldsymbol{R}_0)$$
$$\times \exp\{-{\rm i}(\omega_1+\omega_2)\tau\} \exp\{-\tfrac{1}{2}(\omega_1+\omega_2)^2 T_{\rm s}^2\}, \tag{2.21}$$

where we have evaluated the integral over τ' after writing ψ in terms of its Fourier transform. Now $\overline{\psi}(\omega, \boldsymbol{R}_0)$ cannot contain Fourier components not present in $\bar{F}(\omega)$; thus (cf. (2.2) and (2.3)) $\overline{\psi}(\omega, \boldsymbol{R}_0)$ is zero for all ω except for two narrow bands near $\omega = \omega_0$ and $\omega = -\omega_0$, the bandwidth $\Delta\omega$ being given by the 'uncertainty relation'

$$\Delta\omega \approx c/\sigma. \tag{2.22}$$

These two bands can be separated by writing

$$\overline{\psi}(\omega) = \tfrac{1}{2}(\overline{\psi}_{\rm c}(\omega) + \overline{\psi}_{\rm c}^*(-\omega)). \tag{2.23}$$

The terms $\overline{\psi}_{\rm c}(\omega_1)\,\overline{\psi}_{\rm c}(\omega_2)$ and $\overline{\psi}_{\rm c}^*(-\omega_1)\,\overline{\psi}_{\rm c}^*(-\omega_2)$ contribute to (2.21) with a weighting

$$\exp\{-(\omega_1+\omega_2)^2 T_{\rm s}^2/2\} \approx \exp\{-2\omega_0^2 T_{\rm s}^2\} \approx \exp\{-8\pi^2\}, \tag{2.24}$$

which is negligible, while the cross-terms $\overline{\psi}_{\rm c}(\omega_1)\,\overline{\psi}_{\rm c}^*(-\omega_2)$ and $\overline{\psi}_{\rm c}^*(-\omega_1)\,\overline{\psi}_{\rm c}(\omega_2)$ are weighted by

$$\exp\{-\tfrac{1}{2}(\omega_1+\omega_2)^2 T_{\rm s}^2\} \gtrsim \exp\{-\tfrac{1}{2}(\Delta\omega)^2 T_{\rm s}^2\} \approx \exp\{-\lambda^2/2\sigma^2\}, \tag{2.25}$$

which may be replaced by unity because of the quasi-monochromaticity condition (1.1). Thus (2.21) becomes

$$(\psi^2(\tau, \boldsymbol{R}_0))_{\rm sm} = \frac{1}{4}\int_{-\infty}^{\infty} {\rm d}\omega_1 \int_{-\infty}^{\infty} {\rm d}\omega_2 \exp\{-{\rm i}(\omega_1+\omega_2)\tau\}[\overline{\psi}_{\rm c}(\omega_1)\,\overline{\psi}_{\rm c}^*(-\omega_2) + \overline{\psi}_{\rm c}^*(-\omega_1)\,\overline{\psi}_{\rm c}(\omega_2)], \tag{2.26}$$

from which (2.19) follows immediately.

Since it is generally the smoothed echo whose 'fading' is followed as $\boldsymbol{R}_0$ is varied, much of the rest of this paper will be concerned with the statistics of $|\psi_{\rm c}(\tau, \boldsymbol{R}_0)|$, which we shall henceforth call the echo *amplitude*, and the smoothed power $\frac{1}{2}|\psi_{\rm c}(\tau, \boldsymbol{R}_0)|^2$. Since the amplitude is important from a theoretical point of view, we point out that as well as being given approximately by (2.19), it may be observed very simply as the *envelope* of the curves of $\psi(\tau, \boldsymbol{R}_0)$ against τ which are obtained by varying the phase of the carrier wave $\exp\{-{\rm i}\omega_0 t\}$.

3. Statistical description of rough surfaces

In order to calculate ensemble averages of the echo wavefunction $\psi(\tau, \boldsymbol{R}_0)$ given by (2.12), it is necessary to discuss the *probability distributions* of $f(\boldsymbol{R})$ and $Z(\boldsymbol{R})$. We deal first with $f(\boldsymbol{R})$, leaving $Z(\boldsymbol{R})$ till §3(iii); our treatment is based on that given by Beckmann & Spizzichino (1963, p. 185). *The one-position distribution*, $P_1^f(f)$, is defined by

$$P_1^f(f)\,{\rm d}f \equiv \text{probability that at a point } \boldsymbol{R} \text{ in the 'neighbourhood' beneath the source-receiver the surface height lies between } f \text{ and } f+{\rm d}f. \tag{3.1}$$

With the aid of $P_1^f(f)$ it is possible to take the ensemble average $\langle g(f)\rangle$ of any function $g(f(\boldsymbol{R}))$ of the surface height at a single place $\boldsymbol{R}$; the average is given by

$$\langle g(f)\rangle = \int_{-\infty}^{\infty} \mathrm{d}f P_1^f(f)\, g(f). \tag{3.2}$$

We shall require the Fourier transform

$$\bar{P}_1^f(k) \equiv \langle \exp\{\mathrm{i}kf\}\rangle = \int_{-\infty}^{\infty} \mathrm{d}f \exp\{\mathrm{i}kf\} P_1^f(f). \tag{3.3}$$

A simple parameter of the surface which can be derived from $P_1^f(f)$ is the *r.m.s. height* S, defined by

$$S^2 \equiv \langle f^2\rangle = \int_{-\infty}^{\infty} \mathrm{d}f f^2 P_1^f(f). \tag{3.4}$$

As a model, we shall often take the Gaussian distribution

$$P_1^f(f) = \frac{1}{(2\pi)^{\frac{1}{2}} S} \exp\{-f^2/2S^2\}, \tag{3.5}$$

for which the *mean height* $\langle f\rangle$ is zero as required by our definition of the reference plane.

The function $P_1^f(f)$ does not specify the surface sufficiently for our purposes, because in calculating $\langle \psi^2(\tau, \boldsymbol{R}_0)\rangle$ it will be necessary to take averages over functions $G(f(\boldsymbol{R}_1), f(\boldsymbol{R}_2))$ of the surface at two different places $\boldsymbol{R}_1$ and $\boldsymbol{R}_2$. We therefore require the *two-position distribution* $P_2^f(f_1, f_2, \boldsymbol{R}_2 - \boldsymbol{R}_1)$, defined by

$$P_2^f(f_1, f_2, \boldsymbol{R}_2 - \boldsymbol{R}_1)\, \mathrm{d}f_1 \mathrm{d}f_2 \equiv \text{probability that height at } \boldsymbol{R}_1 \text{ lies between } f_1 \text{ and } f_1 + \mathrm{d}f_1 \textit{ and} \text{ height at } \boldsymbol{R}_2 \text{ lies between } f_2 \text{ and } f_2 + \mathrm{d}f_2. \tag{3.6}$$

In this paper we shall confine ourselves to statistically isotropic surfaces, where only the modulus $|\boldsymbol{R}_2 - \boldsymbol{R}_1| \equiv |\boldsymbol{R}|$ appears in P_2^f. The average value of a function of two positions is

$$\langle G(f(\boldsymbol{R}_1), f(\boldsymbol{R}_2))\rangle = \int_{-\infty}^{\infty} \mathrm{d}f_1 \int_{-\infty}^{\infty} \mathrm{d}f_2 P_2^f(f_1, f_2, \boldsymbol{R}_2 - \boldsymbol{R}_1)\, G(f_1, f_2). \tag{3.7}$$

The Fourier transform of P_2^f is

$$\bar{P}_2^f(k_1, k_2, \boldsymbol{R}) \equiv \langle \exp\{\mathrm{i}(k_1 f(\boldsymbol{R}_1) - k_2 f(\boldsymbol{R}_2))\}\rangle = \int_{-\infty}^{\infty} \mathrm{d}f_1 \int_{-\infty}^{\infty} \mathrm{d}f_2 \exp\{\mathrm{i}(k_1 f_1 - k_2 f_2)\} P_2^f(f_1, f_2, \boldsymbol{R}). \tag{3.8}$$

The distribution $P_1^f(f)$ can be regained from $P_2^f(f_1, f_2, \boldsymbol{R})$ by the relations

$$P_1^f(f) = \int_{-\infty}^{\infty} \mathrm{d}f_2 P_2^f(f, f_2, \boldsymbol{R}) = \frac{1}{2\pi} \int_{-\infty}^{\infty} \mathrm{d}k \exp\{-\mathrm{i}kf\} \bar{P}_2^f(k, 0, \boldsymbol{R}). \tag{3.9}$$

Information about the *correlations* between different points on the surface is provided by the dependence of $P_2^f(f_1, f_2, \boldsymbol{R})$ on $\boldsymbol{R}$. It is easy to see that the complete correlation which must exist for non-pathological surfaces when $|\boldsymbol{R}| = 0$ (i.e. $\boldsymbol{R}_1 = \boldsymbol{R}_2$), together with the complete lack of correlation when $|\boldsymbol{R}| \to \infty$, requires the limiting behaviour

$$P_2^f(f_1, f_2, \boldsymbol{R}) \begin{cases} \xrightarrow{|\boldsymbol{R}| \to 0} & P_1^f(f_1)\, \delta(f_1 - f_2) \\ \xrightarrow{|\boldsymbol{R}| \to \infty} & P_1^f(f_1)\, P_1^f(f_2) \end{cases} \tag{3.10}$$

The *autocorrelation function* of the surface, $C_f(\boldsymbol{R})$ is defined by

$$C_f(\boldsymbol{R}) \equiv \frac{\langle f(\boldsymbol{R}_1) f(\boldsymbol{R}_1+\boldsymbol{R})\rangle}{\langle f^2\rangle}, \tag{3.11}$$

where we have taken account of the fact that $\langle f\rangle$ is zero, and where

$$\langle f(\boldsymbol{R}_1) f(\boldsymbol{R}_1+\boldsymbol{R})\rangle = \int_{-\infty}^{\infty} \mathrm{d}f_1 \int_{-\infty}^{\infty} \mathrm{d}f_2 f_1 f_2 P_2^f(f_1, f_2, \boldsymbol{R}) = \lim_{(k_1,k_2\to 0)} \frac{\partial^2}{\partial k_1 \partial k_2} \bar{P}_2^f(k_1, k_2, \boldsymbol{R}). \tag{3.12}$$

This definition ensures that the limiting behaviour of $C_f(\boldsymbol{R})$ is

$$C_f(\boldsymbol{R}) \begin{cases} \xrightarrow{|\boldsymbol{R}|\to 0} 1 \\ \xrightarrow{|\boldsymbol{R}|\to\infty} 0 \end{cases} \tag{3.13}$$

Given the function $P_2^f(f_1, f_2, \boldsymbol{R})$, a measure of the horizontal scale of the irregularities can be calculated; this is N_f, the average number of times the surface crosses unit length of a straight line in the reference plane, i.e. the *linear density of zero-crossings*. Consider the infinitesimal line-segment joining points $\boldsymbol{R}_1$ and $\boldsymbol{R}_1+\mathrm{d}\boldsymbol{R}_1$ in the reference plane. The surface will cut this line if $f(\boldsymbol{R}_1)$ is negative and $f(\boldsymbol{R}_1+\mathrm{d}\boldsymbol{R}_1)$ is positive, or if $f(\boldsymbol{R}_1)$ is positive and $f(\boldsymbol{R}_1+\mathrm{d}\boldsymbol{R}_1)$ is negative; the probability of this is

$$2\int_{-\infty}^{0} \mathrm{d}f_1 \int_{0}^{\infty} \mathrm{d}f_2 P_2^f(f_1, f_2, \mathrm{d}\boldsymbol{R}),$$

so that the mean number of crossings in unit length, i.e. N_f is

$$N_f = \lim_{\mathrm{d}\boldsymbol{R}\to 0} \frac{2}{|\mathrm{d}\boldsymbol{R}|} \int_{-\infty}^{0} \mathrm{d}f_1 \int_{0}^{\infty} \mathrm{d}f_2 P_2^f(f_1, f_2, \mathrm{d}\boldsymbol{R}). \tag{3.14}$$

Finally, the *distribution of slopes*, $\Pi(f')$, defined as

$$\Pi(f')\,\mathrm{d}f' \equiv \text{probability that the surface gradient at a given point lies between } f' \text{ and } f'+\mathrm{d}f' \tag{3.15}$$

is given in terms of $P_2^f(f_1, f_2, \boldsymbol{R})$ by

$$\left.\begin{aligned} \Pi(f') &= \lim_{R\to 0} R \int_{-\infty}^{\infty} \mathrm{d}f P_2^f(f, f+Rf', R), \\ &= \lim_{R\to 0} R \int_{-\infty}^{\infty} \mathrm{d}k \exp\{\mathrm{i}kRf'\} \bar{P}_2^f(k, k, R). \end{aligned}\right\} \tag{3.16}$$

The machinery has now been developed to enable the three rough surfaces to be defined, for which we shall later calculate average properties of the echo. The first two surfaces have identical $P_1^f(f)$ functions, but different $P_2^f(f_1, f_2, R)$ functions leading to very different slope distributions $\Pi(f')$, so that the surfaces differ qualitatively.

3 (i). *Undulating surface (denoted by α)*

This is the 'Gaussian rough surface' most frequently employed in theoretical discussions (see, for example, Beckmann & Spizzichino 1963, p. 190; Longuet-Higgins 1956). $P_2(f_1, f_2, \boldsymbol{R})$ is defined as

$$P_2^f(f_1, f_2, \boldsymbol{R}) \equiv \frac{1}{2\pi S^2[1-C_f^2(\boldsymbol{R})]^{\frac{1}{2}}} \exp\left\{-\frac{[f_1^2+f_2^2-2f_1 f_2 C_f(\boldsymbol{R})]}{2S^2(1-C_f^2(\boldsymbol{R}))}\right\}, \tag{3.17}$$

a function whose Fourier transform is

$$\bar{P}_2^f(k_1, k_2, \boldsymbol{R}) = \exp\{-\tfrac{1}{2}S^2[k_1^2 + k_2^2 - 2k_1 k_2 C_f(\boldsymbol{R})]\}. \tag{3.18}$$

It is readily verified that this probability distribution satisfies the conditions (3.9) to (3.12), thus representing a possible surface, and that S is the r.m.s. height. For the density of zero-crossings N_f, (3.14) gives

$$N_f = \frac{1}{\pi}[-C_f''(0)]^{\frac{1}{2}}, \tag{3.19}$$

a result also derived by Rice (1945, p. 51) using a different method. It is convenient (although not necessary) to take the model

$$C_f(R) = \exp\{-R^2/L^2\}, \tag{3.20}$$

so that

$$N_f = \frac{2^{\frac{1}{2}}}{\pi L} = \frac{0.450}{L}, \tag{3.21}$$

corresponding to a diameter of about $4L$ for a typical irregularity. For the slope distribution $\Pi(f')$, (3.16) gives

$$\Pi(f') = \frac{L}{S\pi^{\frac{1}{2}}} \exp\{-L^2 f'^2/4S^2\}, \tag{3.22}$$

which is also Gaussian, the r.m.s. slope being $2^{\frac{1}{2}}S/L$.

When reflexion from this surface has been studied before (Beckmann & Spizzichino 1963, pp. 80 ff.), considerable analytical difficulties have been encountered because of the 'exponential of an exponential' which appears in (3.18) if the model (3.20) is used. We avoid these problems by the substitution

$$\exp[S^2 k_1 k_2 \exp\{-R^2/L^2\}] \to (\exp\{S^2 k_1 k_2\} - 1) \exp\left\{-\frac{R^2 S^2 k_1 k_2}{L^2(1 - \exp\{-S^2 k_1 k_2\})}\right\} + 1, \tag{3.23}$$

which has been chosen because it has the correct limiting forms near $R = 0$ and at $R = \infty$, and the correct analytical form for all R when $|S^2 k_1 k_2|$ is small. The substitution is tantamount to replacing $P_2(f_1, f_2, \boldsymbol{R})$ (equation (3.17)) by a different surface probability function, which, although it cannot easily be evaluated in closed form, can nevertheless be shown to have the remarkable property of being identical to (3.17) so far as the quantities $P_1^f(f)$ (equation (3.5)), $C_f(R)$ (equation (3.20)), $\Pi(f')$ (equation (3.22)) and N_f (equation (3.21)) are concerned.

3 (ii). *Surface of steps (denoted by β)*

This has perhaps the simplest two-position probability distribution compatible with (3.9) to (3.12), namely

$$P_2^f(f_1, f_2, \boldsymbol{R}) \equiv P_1^f(f_1)\,\delta(f_1 - f_2)\,C_f(\boldsymbol{R}) + P_1^f(f_1)\,P_1^f(f_2)\,[1 - C_f(\boldsymbol{R})], \tag{3.24}$$

whose Fourier transform is

$$\bar{P}_2^f(k_1, k_2, \boldsymbol{R}) = \exp\{-\tfrac{1}{2}S^2(k_1 - k_2)^2\}\,C_f(\boldsymbol{R}) + \exp\{-\tfrac{1}{2}S^2(k_1^2 + k_2^2)\}\,[1 - C_f(\boldsymbol{R})] \tag{3.25}$$

(the model (3.5) has been used). The nature of this surface is best seen by evaluating $\Pi(f')$; (3.16) gives

$$\Pi(f') = \delta(f') \tag{3.26}$$

so that here, in contrast to the undulating surface, the slope is always zero except possibly at a set of points with measure zero. The surface therefore consists of flat regions separated by vertical walls whose r.m.s. height is $2S$. The density of zero-crossings given by (3.14) is

$$N_f = -\tfrac{1}{2}C_f'(0). \tag{3.27}$$

This means that the model (3.20) cannot be used, and it is not hard to convince oneself (e.g. by considering a one-dimensional function consisting of a series of rectangular hills) that $C_f(R)$ must have a finite slope at the origin for this type of surface. Therefore we employ the model

$$C_f(R) = \exp\{-R/L\}, \tag{3.28}$$

so that

$$N_f = 1/2L, \tag{3.29}$$

which again corresponds to a diameter of about $4L$ for a typical irregularity.

3 (iii). *Flat surface of varying reflectivity (denoted by γ)*

Since $f(\boldsymbol{R})$ is zero, the surface is specified by the statistics of $Z(\boldsymbol{R})$. This function, which is always less than unity, appears only linearly in the basic diffraction integral (2.12), and hence quadratically in the echo power $\psi^2(\tau, \boldsymbol{R}_0)$. Thus the full probability distributions of $Z(\boldsymbol{R})$ are not required; the only relevant quantities are the *mean value* $\langle Z\rangle$ and *mean square value* $\langle Z^2\rangle$, which satisfy

$$\langle Z\rangle^2 \leqslant \langle Z^2\rangle \leqslant 1, \tag{3.30}$$

and the *reflectivity autocorrelation function* $C_Z(\boldsymbol{R})$ defined by

$$C_Z(\boldsymbol{R}) \equiv \frac{\langle Z(\boldsymbol{R}_1)\, Z(\boldsymbol{R}_1+\boldsymbol{R})\rangle - \langle Z\rangle^2}{\langle Z^2\rangle - \langle Z\rangle^2} \tag{3.31}$$

for which we may use either of the models (3.20) and (3.28).

In the polar ice radar experiments (Robin *et al.* 1969), the surface α of § 3 (i) might correspond to an undulating rock glacier bed, or to rugged floating sea ice, the surface β of § 3 (ii) might correspond to the ice/water interface between flat ice floes, while the surface γ of § 3 (iii) might refer to a flat glacier bed made up of various rock types.

4. Statistics of the echo

4 (i). *The distribution of the echo wavefunction*

With the aid of the surface probability distributions of § 3, and the diffraction theory of § 2, we shall be able to calculate the ensemble averages of $\psi(\tau, \boldsymbol{R}_0)$ and $\psi^2(\tau, \boldsymbol{R}_0)$, and the autocorrelation function of the echo wavefunction at two source-receiver positions separated by $\boldsymbol{R}$, defined by

$$C_\psi(\tau, \boldsymbol{R}) \equiv \frac{\langle \psi(\tau, \boldsymbol{R}_0)\, \psi(\tau, \boldsymbol{R}_0+\boldsymbol{R})\rangle - \langle \psi(\tau, \boldsymbol{R}_0)\rangle^2}{\langle \psi^2(\tau, \boldsymbol{R}_0)\rangle - \langle \psi(\tau, \boldsymbol{R}_0)\rangle^2} \tag{4.1}$$

(this quantity is independent of $\boldsymbol{R}_0$). The results, which will be derived in § 5, are essentially exact under the restrictions (1.1) to (1.4). But it is not possible to calculate *directly* the mean values of other quantities, such as the amplitude $|\psi_c(\tau, \boldsymbol{R}_0)|$ (whose significance in terms of smoothing was explained in § 2 (ii)), or the autocorrelation function of ψ^2 rather than ψ; this is because such direct calculations would not only be impossibly complicated, but would involve the unknown many-position probability distributions of the surface height as well as $P_1^f(f)$ and $P_2^f(f_1, f_2, \boldsymbol{R})$ (cf. Mercier (1962) who treats a relatively simple case where the surface is Gaussian and the waves monochromatic).

In a large class of cases, however, this difficulty does not arise, because the complete probability distribution of $\psi(\tau, \boldsymbol{R}_0)$ (considered as a random function of $\boldsymbol{R}_0$ for fixed τ) is known, from which

the ensemble average of any quantity associated with the echo can be calculated. This situation arises whenever the annulus (figure 2) containing surface points which contribute to the echo at a given delay time contains a large number of irregularities, i.e. (equations (2.15), (2.16)), whenever

$$\frac{2\pi R(\tau)\,\Delta R(\tau)}{L^2} = \frac{\pi h\sigma}{L^2} \gg 1. \tag{4.2}$$

Then ψ is the sum of a large number of independent random contributions, so that according to the central limit theorem of probability theory its distribution must be Gaussian, whatever the statistical nature of the underlying rough surface. (One case where (4.2) is obviously violated is that of a surface which varies so gently that it may be considered as a flat plane in the 'neighbourhoods' seen by each source position $\boldsymbol{R}_0$.)

Let us introduce the real random variables ξ, η, ρ, χ by the definitions

$$\psi_c(\tau, \boldsymbol{R}_0) \equiv \rho\, e^{i\chi} \equiv \xi + i\eta, \tag{4.3}$$

so that ξ and ρ are new names for the echo wavefunction and amplitude respectively. According to the central limit theorem, the two-position probability distribution of ξ is

$$P_2^{\xi}(\xi_1, \xi_2, \boldsymbol{R}) \equiv (\text{probability that the echo wavefunction at any source-receiver point } \boldsymbol{R}_0 \text{ lies between } \xi_1 \text{ and } \xi_1 + d\xi_1, \textit{ and} \text{ the wavefunction at the source-receiver point } \boldsymbol{R}_0 + \boldsymbol{R} \text{ lies between } \xi_2 \text{ and } \xi_2 + d\xi_2) \div (d\xi_1\, d\xi_2), \tag{4.4}$$

$$= \frac{\exp\left\{\dfrac{(\xi_1 - \langle\xi\rangle)^2 + (\xi_2 - \langle\xi\rangle)^2 - 2C_{\xi}(\boldsymbol{R})\,(\xi_1 - \langle\xi\rangle)\,(\xi_2 - \langle\xi\rangle)}{2\Sigma_{\xi}(1 - C_{\xi}(\boldsymbol{R}))}\right\}}{2\pi\Sigma_{\xi}(1 - C_{\xi}^2(\boldsymbol{R}))^{\frac{1}{2}}} \tag{4.5}$$

(cf. 3.17). It is easily verified by integration that the single-position distribution $P_1^{\xi}(\xi)$ is a simple Gaussian centred on $\langle\xi\rangle$ with variance Σ_{ξ}, namely

$$P_1^{\xi}(\xi) = \frac{\exp\left\{-\dfrac{(\xi - \langle\xi\rangle)^2}{2\Sigma_{\xi}}\right\}}{(2\pi\Sigma_{\xi})^{\frac{1}{2}}}, \tag{4.6}$$

where

$$\Sigma_{\xi} = \langle\xi^2\rangle - \langle\xi\rangle^2, \tag{4.7}$$

and that $C_{\xi}(\boldsymbol{R})$ is identical with $C_{\psi}(\tau, \boldsymbol{R}_0)$ defined by (4.1). It should be remembered that Σ, $\langle\xi\rangle$ etc. depend on τ; for convenience of writing this dependence has been left implicit.

The echo is said to be *incoherent* if $\Sigma_{\xi} \gg \langle\xi\rangle^2$, and *coherent* if $\Sigma_{\xi} \ll \langle\xi\rangle^2$. A very clear general discussion of these terms is given by Beckmann & Spizzichino (1963, chap. 7.3). We shall show in §5 that the echo is always incoherent in its 'tail' (i.e. for delay times τ exceeding $\sigma/2c$), and whenever the surface height S exceeds about $\frac{1}{8}\lambda$ – i.e. only the head of the echo from a nearly perfect flat mirror is coherent.

To illustrate the usefulness of the distribution $P_2^{\xi}(\xi_1, \xi_2, \boldsymbol{R})$ we calculate two quantities characterizing the spatial fading of the echo. First, the average number of times the echo wavefunction passes through its mean value when the source traverses unit length of a horizontal straight line, $N_{\xi}(\langle\xi\rangle)$ can be shown by an argument similar to that leading to (3.14), to be given by

$$N_{\xi}(\langle\xi\rangle) = \lim_{|d\boldsymbol{R}|\to 0} \frac{2}{|d\boldsymbol{R}|} \int_{-\infty}^{\langle\xi\rangle} d\xi_1 \int_{\langle\xi\rangle}^{\infty} d\xi_2\, P_2^{\xi}(\xi_1, \xi_2, d\boldsymbol{R}). \tag{4.8}$$

This can be evaluated by using (4.5), to give

$$N_\xi(\langle\xi\rangle) = (1/\pi)\,[-C_\xi''(0)]^{\frac{1}{2}}. \tag{4.9}$$

Secondly, the autocorrelation function of the (unsmoothed) power, $C_{\xi^2}(\boldsymbol{R})$, defined by

$$C_{\xi^2}(\boldsymbol{R}) \equiv \frac{\langle\xi_1^2\xi_2^2\rangle - \langle\xi^2\rangle^2}{\langle\xi^4\rangle - \langle\xi^2\rangle^2}, \tag{4.10}$$

where the subscripts 1 and 2 denote source points separated by R, can also be evaluated by using (4.5). We write ξ_1, or ξ_2 as

$$\xi_{1,2} = (\xi_{1,2} - \langle\xi\rangle) + \langle\xi\rangle \tag{4.11}$$

in (4.10), and use the results (which can be obtained from (4.5) and (4.6)), that

$$C^{(\boldsymbol{R})}_{(\xi-\langle\xi\rangle)^2} \equiv \frac{\langle(\xi_1-\langle\xi\rangle)^2(\xi_2-\langle\xi\rangle)^2\rangle - \Sigma_\xi^2}{\langle(\xi-\langle\xi\rangle)^4\rangle - \Sigma_\xi^2} = C_\xi^2(\boldsymbol{R}), \tag{4.12}$$

and

$$\langle(\xi-\langle\xi\rangle)^4\rangle = 3\Sigma_\xi^2. \tag{4.13}$$

Tedious algebra then gives

$$C_{\xi^2}(\boldsymbol{R}) = \frac{C_\xi^2(\boldsymbol{R}) + (2\langle\xi\rangle^2/\Sigma_\xi)\,C_\xi(\boldsymbol{R})}{1 + 2\langle\xi\rangle^2/\Sigma_\xi}, \tag{4.14}$$

a formula whose dependence on $\langle\xi\rangle^2/\Sigma_\xi$ shows the effect of the coherence of the echo, the limiting values being

$$C_{\xi^2}(\boldsymbol{R}) \begin{cases} \xrightarrow{\text{coherent}} C_\xi(\boldsymbol{R}) \\ \xrightarrow{\text{incoherent}} C_\xi^2(\boldsymbol{R}) \end{cases} \tag{4.10}$$

4 (ii). *The distribution of the echo amplitude*

The wavefunction ξ whose distribution is given by (4.5) is often not a convenient quantity for experimental study. In order to measure the spatial fading rate $N_\xi(\langle\xi\rangle)$ (equation (4.9)), for instance, great care must be taken to keep the delay time very accurately fixed; because ξ is not a 'smoothed' quantity in the sense of § 2 (ii), any errors in τ comparable with a carrier-wave period would introduce oscillations in addition to those produced by true spatial fading, leading to an incorrect measurement of $N_\xi(\langle\xi\rangle)$. The quantity whose probability distribution is commonly required in the interpretation of experiments is not ξ but the amplitude ρ, whose square gives the smoothed power as discussed in § 2 (ii).

We calculate the distribution of ρ with the aid of (4.3), using the fact that the distribution of η must be Gaussian under the same conditions as that of ξ. The random variables ξ and η are assumed to be *statistically independent*, so that their joint two-position distribution is given by the product

$$P_2^{\xi,\eta}(\xi_1,\xi_2;\eta_1,\eta_2;\boldsymbol{R}) = P_2^{\xi}(\xi_1,\xi_2,\boldsymbol{R})\,P_2^{\eta}(\eta_1,\eta_2,\boldsymbol{R}). \tag{4.16}$$

($P_2^\xi(\xi_1,\xi_2,\boldsymbol{R})$ is given by (4.5).) A detailed discussion of the joint distributions of ξ and η (unfortunately restricted to the single-position case $\boldsymbol{R} = 0$ and therefore unable to deal with spatial fading) is given by Beckmann & Spizzichino (1963, ch. 7); they show that ξ and η are independent if

$$\langle\xi\eta\rangle = \langle\xi\rangle\langle\eta\rangle, \tag{4.17}$$

and that this equation can always be made to hold by changing the phase χ in (4.3) by a suitably chosen angle ϕ_0 (which will depend on τ in our problem). In §5 we shall calculate $\langle\xi\eta\rangle$ and $\langle\xi\rangle\langle\eta\rangle$ and show that (4.17) holds whenever the echo is completely incoherent or completely coherent, and is a very good approximation in all cases for the present problem; thus we shall assume (4.17) always, which greatly simplifies the mathematics. We also assume that the variance Σ_η and the autocorrelation function $C_\eta(\boldsymbol{R})$ are equal to their counterparts for the variable ξ, i.e. that

$$\Sigma_\eta = \Sigma_\xi \equiv \Sigma, \text{ say}, \tag{4.18a}$$

$$C_\eta(\boldsymbol{R}) = C_\xi(\boldsymbol{R}) \equiv C_{\psi_c\psi_c^*}(\boldsymbol{R}), \text{ say} \tag{4.18b}$$

(the notation in the last definition will be explained presently). The mean smoothed power is then given by

$$\langle\rho^2\rangle \equiv \langle\xi^2+\eta^2\rangle = 2\Sigma+\langle\xi\rangle^2+\langle\eta\rangle^2. \tag{4.19}$$

The results of §5 will show that the assumptions (4.18a, b) are justified whenever (4.17) holds – i.e. almost always.

If the correlation function between $\psi_c(\tau, \boldsymbol{R}_0)$ and $\psi_c^*(\tau, \boldsymbol{R}_0+\boldsymbol{R})$ is denoted by $C_{\psi_c\psi_c^*}(\boldsymbol{R})$, this is consistent with (4.18b), because (cf. 4.3)

$$C_{\psi_c\psi_c^*}(\boldsymbol{R}) \equiv \frac{\langle\psi_c(\tau,\boldsymbol{R}_0)\,\psi_c^*(\tau,\boldsymbol{R}_0+\boldsymbol{R})\rangle - |\langle\psi_c(\tau,\boldsymbol{R}_0)\rangle|^2}{\langle|\psi_c(\tau,\boldsymbol{R}_0)|^2\rangle - |\langle\psi_c(\tau,\boldsymbol{R}_0)\rangle|^2} \tag{4.20}$$

$$= \frac{\langle(\xi_1+i\eta_1)\,(\xi_2-i\eta_2)\rangle - |\langle\xi\rangle+i\langle\eta\rangle|^2}{\langle(\xi^2+\eta^2)\rangle - |\langle\xi\rangle+i\langle\eta\rangle|^2}$$

$$= \frac{\langle\xi_1\xi_2\rangle - \langle\xi\rangle^2 + \langle\eta_1\eta_2\rangle - \langle\eta\rangle^2}{\langle\xi^2\rangle - \langle\xi\rangle^2 + \langle\eta^2\rangle - \langle\eta\rangle^2}$$

$$= \frac{C_\xi(\boldsymbol{R})\,[\langle\xi^2\rangle - \langle\xi\rangle^2] + C_\eta(\boldsymbol{R})\,[\langle\eta^2\rangle - \langle\eta\rangle^2]}{\langle\xi^2\rangle - \langle\xi\rangle^2 + \langle\eta^2\rangle - \langle\eta\rangle^2}, \tag{4.21}$$

implying the second equality in (4.18b) if the first holds. The autocorrelation function $C_{\rho^2}(\boldsymbol{R})$ of the smoothed power – a quantity readily amenable to experiment – can be calculated in a similar manner to $C_{\xi^2}(\boldsymbol{R})$ (equation (4.14)); we obtain

$$C_{\rho^2}(\boldsymbol{R}) \equiv \frac{\langle\rho_1^2\rho_2^2\rangle - \langle\rho^2\rangle^2}{\langle\rho^4\rangle - \langle\rho^2\rangle^2}, \tag{4.22}$$

$$= \frac{C_{\psi_c\psi_c^*}^2(\boldsymbol{R}) + C_{\psi_c\psi_c^*}(\boldsymbol{R})\,(\langle\xi\rangle^2+\langle\eta\rangle^2)/\Sigma}{1+\{\langle\xi\rangle^2+\langle\eta\rangle^2\}/\Sigma}. \tag{4.23}$$

The general two-position probability distribution of the amplitude ρ is obtained by transforming (4.16) to polar coordinates with the aid of (4.3), and integrating over the phases χ, i.e.

$$P_2^\rho(\rho_1,\rho_2,\boldsymbol{R}) = \rho_1\rho_2\int_0^{2\pi} d\chi_1 \int_0^{2\pi} d\chi_2 P_2^\xi(\rho_1\cos\chi_1, \rho_2\cos\chi_2, \boldsymbol{R})\, P_2^\eta(\rho_1\sin\chi_1, \rho_2\sin\chi_2, \boldsymbol{R}). \tag{4.24}$$

This cannot be evaluated in simple closed form, but the following important results can be derived from it:

(*a*) *The one-position distribution* $P_1^\rho(\rho)$ can be found, by integrating (4.24) over one of the ρ-variables, to be

$$P_1^\rho(\rho) = \frac{\rho}{\Sigma}\exp\left\{-\frac{(\rho^2+\langle\xi\rangle^2+\langle\eta\rangle^2)}{2\Sigma}\right\} I_0\left(\frac{\rho}{\Sigma}\sqrt{(\langle\xi\rangle^2+\langle\eta\rangle^2)}\right), \tag{4.25}$$

where I_0 is the modified Bessel function of the first kind. This is the distribution of a 'constant vector + random vector', originally derived by Rice (1945, p. 100); as a simple check, $\langle\rho^2\rangle$ may be evaluated, and the result (4.19) is obtained.

(*b*) In the commonly occurring case of a *completely incoherent echo*, when $\langle\xi\rangle^2$ and $\langle\eta\rangle^2$ are negligible in comparison with Σ, (4.24) becomes

$$P_2^\rho(\rho_1,\rho_2,\boldsymbol{R}) \xrightarrow[\text{echo}]{\text{incoherent}} \frac{\rho_1\rho_2\exp\left\{-\dfrac{(\rho_1^2+\rho_2^2)}{2\Sigma(1-C^2_{\psi_c\psi_c^*}(\boldsymbol{R}))}\right\}}{\Sigma^2(1-C^2_{\psi_c\psi_c^*}(\boldsymbol{R}))} I_0\left[\frac{C^2_{\psi_c\psi_c^*}(\boldsymbol{R})\,\rho_1\rho_2}{\Sigma(1-C^2_{\psi_c\psi_c^*}(\boldsymbol{R}))}\right], \tag{4.26}$$

a result also derived by Rice (1945, p. 78). The one-position amplitude distribution for this important case is the Rayleigh distribution,

$$P_1^\rho(\rho) \xrightarrow[\text{echo}]{\text{incoherent}} (\rho/\Sigma)\exp\{-\rho^2/2\Sigma\}, \tag{4.27}$$

which follows at once from (4.25).

(*c*) *The autocorrelation function* $C_\rho(\boldsymbol{R})$ of the amplitude has been evaluated by Booker *et al.* (1950); using (4.26), they show that, to a very close approximation,

$$C_\rho(\boldsymbol{R}) \equiv \frac{\langle\rho_1\rho_2\rangle-\langle\rho\rangle^2}{\langle\rho^2\rangle-\langle\rho\rangle^2} \xrightarrow[\text{echo}]{\text{incoherent}} C^2_{\psi_c\psi_c^*}(\boldsymbol{R}). \tag{4.28}$$

However, this is also the 'incoherent' limit of the expression (4.23) for $C_{\rho^2}(\boldsymbol{R})$ and we conjecture

$$C_\rho(\boldsymbol{R}) \approx C_{\rho^2}(\boldsymbol{R}) \tag{4.29}$$

in all cases. To test this conjecture, the autocorrelations of some powers of ξ, which has the Gaussian distribution (4.5), have been calculated. For the two functions ξ and ξ^3, both of which may take positive or negative values, we find

$$C_\xi - C_{\xi^3} \leqslant 0.14, \tag{4.30}$$

while for the two positive functions ξ^2 and ξ^4 (somewhat analogous to ρ and ρ^2) we find

$$C_{\xi^2} - C_{\xi^4} \leqslant 0.0625. \tag{4.31}$$

(*d*) *The distribution of the spatial rates of change of* ρ can be calculated from (4.24) using the relations

$$\Pi(\rho,\rho') \equiv (\text{probability that the fading rate } \rho' \equiv \partial\rho(\tau,\boldsymbol{R})/\partial|\boldsymbol{R}| \text{ lies between } \rho' \text{ and } \rho'+\mathrm{d}\rho' \textit{ and} \text{ the amplitude lies between } \rho \text{ and } \rho+\mathrm{d}\rho) \div (\mathrm{d}\rho\,\mathrm{d}\rho'), \tag{4.32}$$

$$= \lim_{|\mathrm{d}\boldsymbol{R}|\to 0} |\mathrm{d}\boldsymbol{R}|\, P_2^\rho(\rho,\rho+\rho'\,|\mathrm{d}\boldsymbol{R}|,\mathrm{d}\boldsymbol{R}). \tag{4.33}$$

The limit, which is evaluated in appendix 1, yields

$$\Pi(\rho,\rho') = \frac{P_1^\rho(\rho)\exp\{-\rho'^2/2\Sigma[-C''_{\psi_c\psi_c^*}(0)]\}}{[-2\pi\Sigma C''_{\psi_c\psi_c^*}(0)]^{\frac{1}{2}}}, \tag{4.34}$$

where $P_1^\rho(\rho)$ is the Rice distribution (4.25). This means that ρ and ρ' are independent random functions, and the fading rate satisfies a Gaussian distribution, whose r.m.s. value is

$$\langle\rho'^2\rangle^{\frac{1}{2}} = [-\Sigma C''_{\psi_c\psi_c^*}(0)]^{\frac{1}{2}}. \tag{4.35}$$

We shall make use of this result in §7 (ii) to derive the ultimate positional sensitivity of echo-location.

(*e*) *Rate of crossing a given amplitude level.* The waxing and waning of the amplitude ρ as the source position $\boldsymbol{R}_0$ varies (with τ kept fixed) can be described by

$$N_\rho(\rho_0) = \text{average number of times that } \rho \text{ passes through a datum level } \rho_D \text{ when the source traverses unit length of a horizontal straight line,} \tag{4.36}$$

$$= \lim_{|\mathrm{d}\boldsymbol{R}|\to 0} \frac{2}{|\mathrm{d}\boldsymbol{R}|} \int_0^{\rho_D} \mathrm{d}\rho_1 \int_{\rho_D}^{\infty} \mathrm{d}\rho_2 P_2^\rho(\rho_1, \rho_2, \mathrm{d}\boldsymbol{R}). \tag{4.37}$$

This double integral is evaluated in appendix 1; the result is

$$N_\rho(\rho_D) = P_1^\rho(\rho_D) \left[\frac{-2\Sigma C''_{\psi_c \psi_c^*}(0)}{\pi}\right]^{\frac{1}{2}}. \tag{4.38}$$

As expected, the fading rate is very small if ρ_D is very large or very small, since it is unlikely that the amplitude would reach such a level. The fastest fading rate occurs when $P_1^\rho(\rho_D)$ is a maximum, and a study of (4.25) shows that this maximum rate varies with the degree of coherence. The fastest fading rate of all occurs when the echo is completely incoherent; the corresponding datum level is

$$\rho_D^{\max} = \Sigma^{\frac{1}{2}} \tag{4.39}$$

(i.e. $1/\sqrt{2}$ of the r.m.s. value of ρ, cf. (4.19)), and the maximum fading rate is

$$N_\rho^{\max} = \left[\frac{-2C''_{\psi_c \psi_c^*}(0)}{\pi \mathrm{e}}\right]^{\frac{1}{2}}. \tag{4.40}$$

5. Calculation of averages

We have found in §4 that, under the commonly satisfied condition (4.2), all the statistical properties of the echo can be derived from the two ensemble averages

$$\langle \rho \mathrm{e}^{\mathrm{i}\chi} \rangle_\tau \equiv \langle \psi_c(\tau, \boldsymbol{R}_0) \rangle \tag{5.1}$$

(which is independent of $\boldsymbol{R}_0$), and

$$\langle \rho_1 \exp\{\mathrm{i}\chi_1\} \rho_2 \exp\{-\mathrm{i}\chi_2\} \rangle_\tau \equiv \langle \psi_c(\tau, \boldsymbol{R}_0)\, \psi_c^*(\tau, \boldsymbol{R}_0 + \boldsymbol{R}) \rangle \tag{5.2}$$

(which depends on $\boldsymbol{R}$ but not $\boldsymbol{R}_0$). In this section we shall employ the diffraction theory of §2.1 to calculate these averages and, in addition, the averages $\langle \xi\eta \rangle$, $\langle \xi^2 \rangle$ and $\langle \eta^2 \rangle$ which will be used to establish the validity of (4.17) and (4.18), on which much of the simplicity of the results of §4 depends.

5 (i). *Average echo wavefunction*

Considering first the case where the reflectivity is unity (i.e. surfaces α and β of §3), we use (2.12) applied to the complex echo wavefunction; the integrand of this expression involves the surface height $f(\boldsymbol{R})$ at a single point, so that we may perform the averaging with the aid of the single-position probability distribution $P_1^f(f)$ via (3.2). The result is

$$\begin{aligned}
\langle \rho \exp\{\mathrm{i}\chi\} \rangle_\tau &= -\frac{1}{2\pi c h^2} \iint \mathrm{d}\boldsymbol{R} \left\langle F_c'\left(\tau + \frac{2f(\boldsymbol{R})}{c} - \frac{(\boldsymbol{R}-\boldsymbol{R}_0)^2}{ch}\right)\right\rangle \\
&= -\frac{1}{2\pi c h^2} \int_{-\infty}^{\infty} \mathrm{d}f P_1^f(f) \iint \mathrm{d}\boldsymbol{R}\, F_c'\left(\tau + \frac{2f}{c} - \frac{(\boldsymbol{R}-\boldsymbol{R}_0)^2}{ch}\right) \\
&= -\frac{1}{2h} \int_{-\infty}^{\infty} \mathrm{d}f P_1^f(f)\, F_c\left(\tau + \frac{2f}{c}\right) \equiv -\frac{1}{2h} \left\langle F_c\left(\tau + \frac{2f}{c}\right)\right\rangle.
\end{aligned} \tag{5.3}$$

Thus the average echo is a smoothed version of the echo (2.13) which would be received from a perfect mirror; the smoothing function is $P_1^f(f)$ whose extent is governed by the r.m.s. surface height S. Because of the quasimonochromaticity of the outgoing pulse $F(t)$ and $F_c(t)$, this smoothing reduces $\langle\rho\exp\{i\chi\}\rangle_\tau$ to zero whenever S approaches λ. More precisely, the models (2.2 to 2.4) and (3.5) can be used in (5.3), to give the exact result

$$\langle\rho\exp\{i\chi\}\rangle_\tau = -\frac{A\exp\left\{-\dfrac{c^2\tau^2}{\sigma^2(1+8S^2/\sigma^2)}\right\}\exp\left\{-\dfrac{8\pi^2S^2}{\lambda^2(1+8S/^2\sigma^2)}\right\}\exp\left\{-\dfrac{i\omega_0\tau}{1+8S^2/\sigma^2}\right\}}{2h\sqrt{(1+8S^2/\sigma^2)}}. \quad (5.4)$$

The second exponential factor indicates that the average echo wave is reduced to about 30 % of its perfect-mirror value when $S\sim\frac{1}{8}\lambda$, and about 1 % when $S\sim\frac{1}{4}\lambda$. *A fortiori*, $\langle\rho\exp\{i\chi\}\rangle_\tau$ is utterly negligible whenever S approaches σ (cf. 1.1), so that the quantity $8S^2/\sigma^2$ can be neglected throughout (5.4) to give the following simpler expressions, which are valid to a very high degree of approximation:

$$\langle\rho\exp\{i\chi\}\rangle_\tau = -\frac{A}{2h}\exp\{-8\pi^2S^2/\lambda^2\}\exp\{-c^2\tau^2/\sigma^2\}\exp\{-i\omega_0\tau\}$$

$$= -\frac{\exp\{-8\pi^2S^2/\lambda^2\}F_c(\tau)}{2h}. \quad (5.5)$$

The average real wavefunction is

$$\langle\xi\rangle \equiv \langle\psi(\tau, \boldsymbol{R}_0)\rangle = -\frac{\exp\{-8\pi^2S^2/\lambda^2\}F(\tau)}{2h}, \quad (5.6)$$

while

$$\langle\eta\rangle = \operatorname{Im}\langle\psi_c(\tau, \boldsymbol{R}_0)\rangle = -\frac{\exp\{-8\pi^2S^2/\lambda^2\}}{2h}\operatorname{Im}F_c(\tau). \quad (5.7)$$

These results show that the form and duration σ/c of the average echo wavefunction mirror the original pulse. However, the echo received above any *particular* point (i.e. not averaged), generally has a long tail. We may reasonably conjecture that the zeros in this tail are quasi-periodic with the carrier frequency ω_0 but their locations wander over several carrier-wave periods as the source-receiver is moved. Thus the tail in $\langle\xi\rangle$ is washed out by phase averaging, and to investigate the statistics of the asymmetrical broadening of the echo it is necessary to calculate product averages such as $\langle\xi^2\rangle$ or $\langle\rho^2\rangle$; this will be done in §5 (ii). The vanishing of $\langle\xi\rangle$ due to phase averaging, which also occurs in the main body of the echo if $S\gtrsim\frac{1}{8}\lambda$ corresponds to *incoherence* as defined in §4 (i) (following (4.7)).

None of the results of this section involves the two-position surface distribution function $P_2^f(f_1, f_2, \boldsymbol{R})$ defined in (3.6), so that measurements of $\langle\xi\rangle$ can never provide information about the correlations between different parts of the surface. But it is possible, at least in principle, to take advantage of the 'convolution' form of the penultimate member of equation (5.3) to obtain $P_1^f(f)$ in the form

$$P_1^f(f) = -\frac{2h}{\pi c}\int_{-\infty}^{\infty}d\omega\,\frac{\langle\overline{\psi}(\omega, \boldsymbol{R}_0)\rangle\exp\{2i\omega f\}}{\bar{F}(\omega)}. \quad (5.8)$$

As a practical method for determining $P_1^f(f)$ this equation suffers formidable disadvantages, as discussed by Berry (1972) in connexion with the more general 'surface function' $g(r)$ involved in deconvoluting echoes which are not averaged; these disadvantages are due to the quasi-monochromaticity of the incident pulse.

In the case of the flat surface γ (§3(iii)) calculation of $\langle \rho \exp\{i\chi\}\rangle_\tau$ is trivial; we have

$$\langle \rho \exp\{i\chi\}\rangle = -\frac{\langle Z\rangle F_c(\tau)}{2h}, \tag{5.9}$$

and corresponding results for $\langle \xi\rangle$ and $\langle \eta\rangle$, so that once again the average wavefunction has the 'perfect-mirror' form, and the only effect of reflexion at the surface is to reduce the intensity.

5(ii). *Average product of echo wavefunctions for two different source-receiver positions*

The average product (5.2) of the complex wavefunction will be evaluated initially for the two rough surfaces α and β. The first few steps of the argument may be written successively as

$$\langle \rho_1 \exp\{i\chi_1\}\rho_2 \exp\{-i\chi_2\}\rangle_\tau = \frac{1}{4\pi^2 c^2 h^4}\iint d\boldsymbol{R}_1 \iint d\boldsymbol{R}_2 \left\langle F_c'\left(\tau + \frac{2f(\boldsymbol{R}_1)}{c} - \frac{(\boldsymbol{R}_1-\boldsymbol{R}_0)^2}{ch}\right) \times F_c^{*\prime}\left(\tau + \frac{2f(\boldsymbol{R}_2)}{c} - \frac{(\boldsymbol{R}_2-\boldsymbol{R}_0-\boldsymbol{R})^2}{ch}\right)\right\rangle \tag{5.10}$$

$$= \frac{1}{4\pi^2 c^2 h^4}\int_{-\infty}^{\infty} d\omega_1 \int_{-\infty}^{\infty} d\omega_2\, \omega_1\omega_2\, \bar{a}(\omega_1-\omega_0)\, \bar{a}^*(\omega_2-\omega_0) \times \exp\{-i(\omega_1-\omega_2)\tau\}\iint d\boldsymbol{R}_1 \iint d\boldsymbol{R}_2 \times \exp\{(i/hc)(\omega_1 R_1^2 - \omega_2|\boldsymbol{R}_2-\boldsymbol{R}|^2)\} \times \langle \exp\{-(2i/c)(\omega_1 f(\boldsymbol{R}_1) - \omega_2 f(\boldsymbol{R}_2))\}\rangle \tag{5.11}$$

$$= \frac{1}{4\pi^2 c^2 h^4}\int_{-\infty}^{\infty} d\omega_1 \int_{-\infty}^{\infty} d\omega_2\, \omega_1\omega_2\, \bar{a}(\omega_1-\omega_0)\, \bar{a}^*(\omega_2-\omega_0) \times \exp\{-i(\omega_1-\omega_2)\tau\}\iint d\boldsymbol{R}_1 \iint d\boldsymbol{R}_2 \times \exp\{(i/hc)(\omega_1 R_1^2 - \omega_2|\boldsymbol{R}_2-\boldsymbol{R}|^2)\}\bar{P}_2\left(\frac{2\omega_2}{c}, \frac{2\omega_1}{c}, |\boldsymbol{R}_2-\boldsymbol{R}_1|\right) \tag{5.12}$$

$$= \frac{1}{2ch^3}\int_0^{\infty} d\tau' \int_0^{\infty} d\omega_1 \int_0^{\infty} d\omega_2\, \omega_1\omega_2\, \bar{a}(\omega_1-\omega_0)\, \bar{a}^*(\omega_2-\omega_0) \times \exp\{-i(\omega_1-\omega_2)(\tau-\tau')\} J_0\left(2R\sqrt{\frac{\omega_1\omega_2\tau'}{ch}}\right) \times \int_0^{\infty} dR' R' J_0\left(2R'\sqrt{\frac{\omega_1\omega_2\tau'}{ch}}\right)\bar{P}_2\left(\frac{2\omega_2}{c}, \frac{2\omega_1}{c}, R'\right). \tag{5.13}$$

The first equation, (5.10), follows from the basic diffraction integral (2.12). To obtain (5.11) the Fourier representation (2.3) of the pulse envelope $a(\tau)$ has been introduced, and (5.12) has been obtained by using the two-position surface distribution function (3.8). Finally (5.13), involving the dummy delay time variable τ' which labels the different rings of the annulus contributing to the echo at τ (figure 2), can be derived as explained in appendix 2 (we have also restricted ω_1 and ω_2 to positive values, thus incurring an error depending on the tail of the function $\bar{a}(\omega)$ when $\omega > \omega_0$, which can be shown from the model (2.4) to be of order

$$\exp\{-\pi^2\sigma^2/\lambda^2\};$$

this is utterly negligible in view of (1.1)).

To proceed further we must perform the integrals over R' in (5.13). For the surface α we use (3.18) together with the model (3.20) and the substitution (3.23), while for surface β we use (3.25) and the model (3.28). The R'-integrals are standard (see, for example, Gradshteyn & Ryzhik 1965), and the result is

$$\begin{aligned}\langle\rho_1 \exp\{\mathrm{i}\chi_1\}\rho_2 \exp\{-\mathrm{i}\chi_2\}\rangle_\tau = \frac{1}{4h^2}\int_0^\infty \mathrm{d}\omega_1 \int_0^\infty \mathrm{d}\omega_2\, \bar{a}(\omega_1-\omega_0)\,\bar{a}^*(\omega_2-\omega_0)\exp\{-\mathrm{i}(\omega_1-\omega_2)\,\tau\}\\ \times\left\{\exp\{-2S^2(\omega_1^2+\omega_2^2)/c^2\}+\int_0^\infty \mathrm{d}\tau' \exp\{\mathrm{i}(\omega_1-\omega_2)\,\tau'\}\right.\\ \times Q(\omega_1\omega_2,\tau')\,J_0\left(2R\sqrt{\frac{\omega_1\omega_2\tau'}{ch}}\right)\\ \left.\times\left[\exp\{-2S^2(\omega_1-\omega_2)^2/c^2\}-\exp\{-2S^2(\omega_1^2+\omega_2^2)/c^2\}\right]\right\},\end{aligned} \tag{5.14}$$

where

$$Q(\omega_1\omega_2,\tau') = \frac{cL^2}{4S^2}\left(1-\exp\{-4S^2\omega_1\omega_2/c^2\}\right)\exp\left[-\frac{\tau' cL^2}{4S^2h}\left(1-\exp\{-4S^2\omega_1\omega_2/c^2\}\right)\right] \quad \text{(surface } \alpha\text{)}, \tag{5.15}$$

$$= \frac{1}{2}\left[\frac{ch}{4\omega_1\omega_2L^2}\right]^{\frac{1}{2}}\left(\tau'+\frac{ch}{4\omega_1\omega_2L^2}\right)^{-\frac{3}{2}} \quad \text{(surface } \beta\text{)}. \tag{5.16}$$

It is to be noted that

$$\int_0^\infty \mathrm{d}\tau' Q(\omega_1\omega_2,\tau') = 1. \tag{5.17}$$

The final step in arriving at a manageable expression for $\langle\rho_1 \exp\{\mathrm{i}\chi_1\}\rho_2 \exp\{-\mathrm{i}\chi_2\}\rangle_\tau$ is the performance of the integrations over ω_1 and ω_2 in (5.14). We do this by employing the quasi-monochromaticity assumption (1.1), which implies that the pulse envelope $a(t)$ is a slowly-varying function of t so that $\bar{a}(\omega)$ is concentrated near $\omega = 0$, and only the ranges

$$\omega_1 \approx \omega_0, \omega_2 \approx \omega_0$$

contribute significantly to (5.14). More precisely,

$$|\omega-\omega_0| \lesssim c/\sigma \tag{5.18}$$

since σ/c is the pulse duration. To take account of this, we replace $\omega_1^2+\omega_2^2$ by $2\omega_0^2$, and $\omega_1\omega_2$ by ω_0^2 throughout (5.14). A careful analysis of (5.14) reveals that the only place where these substitutions may lead to appreciable error is in the Bessel-function factor when R or τ' are large, and it is necessary to impose the following restriction on the separation R of the two source-receiver positions:

$$R < \Delta R(\tau'), \tag{5.19}$$

where $\Delta R(\tau')$ is given by (2.16). Now, we shall see in § 6 that only values of τ' which are approximately equal to τ contribute to the echo integrals, so that (5.19) has the physical interpretation that the annuli on the surface (figure 2) beneath the two-source-receiver positions must overlap all around their perimeter, and essentially the same surface irregularities contribute to the echo at the two positions. Fortunately, this is not a serious restriction on R, since we shall find in § 7 (i) that the 'fading wavelength' – which gives the scale of the spatial correlations in the echo – is considerably smaller than $\Delta R(\tau)$, and, further, that there is generally no correlation at all between source-receiver points whose separation is as great as $\Delta R(\tau)$. After making these substitutions for $\omega_1^2+\omega_2^2$ and $\omega_1\omega_2$, it is easy to perform the integrations over ω_1 and ω_2 using

elementary theorems of Fourier analysis. The result is

$$\langle \rho_1 \exp\{i\chi_1\} \rho_2 \exp\{-i\chi_2\} \rangle_\tau = |\langle \rho \exp\{i\chi\} \rangle_\tau|^2 + \int_0^\infty d\tau' Q(\omega_0^2, \tau') \times J_0\left(2R\omega_0 \sqrt{\frac{\tau'}{ch}}\right) \left[\frac{\langle a^2(\tau - \tau' + (2f/c)) \rangle}{4h^2} - |\langle \rho \exp\{i\chi\} \rangle_{\tau-\tau'}|^2\right], \tag{5.20}$$

where $\langle \rho \exp\{i\chi\} \rangle_\tau$ is given by (5.5), and

$$\langle a^2(\tau - \tau' + (2f/c)) \rangle = \int_{-\infty}^\infty df P_1^f(f)\, a^2(\tau - \tau' + (2f/c)) = \frac{\exp\left\{-\frac{2(\tau-\tau')^2 c^2}{\sigma^2(1+16S^2/\sigma^2)}\right\}}{\sqrt{(1+16S^2/\sigma^2)}}, \tag{5.21}$$

so that this function closely resembles the original pulse power envelope, broadened only if $S \gtrsim \frac{1}{4}\sigma$.

Equation (5.20) is the central analytical result of this paper; it contains a wealth of physical meaning, which will be explored in §§6 and 7. First, however, it is necessary to tie up some loose ends from §4(ii), namely the investigation of the validity of the statistical assumptions (4.17) and (4.18*a*) (we leave (4.18*b*) to the interested reader – its proof is essentially the same as (4.18*a*)). These two equations are respectively the imaginary and real parts of

$$\langle \rho^2 \exp\{2i\chi\} \rangle_\tau = \langle \rho \exp\{i\chi\} \rangle_\tau^2. \tag{5.22}$$

The arguments which led from (5.10) to (5.20) are easily adapted to this case (which is actually rather simpler, because R is zero) and yield

$$\langle \rho^2 \exp\{2i\chi\} \rangle_\tau - \langle \rho \exp\{i\chi\} \rangle_\tau^2 = \frac{a^2(\tau)}{4h^2} \exp\{-2i\omega_0\tau\} [\exp\{-16\pi^2 S^2/\lambda^2\} - \exp\{-32\pi^2 S^2/\lambda^2\}] \times \frac{i\omega_0}{ch} \int_0^\infty dR' R' \exp\{-iR'^2\omega_0/ch\}\, W(R'), \tag{5.23}$$

where

$$W(R') = \exp\left[-\frac{4S^2\omega_0^2 R'^2}{c^2 L^2(\exp\{4S^2\omega_0^2/c^2\} - 1)}\right] \quad \text{(surface } \alpha\text{)}, \qquad = \exp\{-R'/L\} \quad \text{(surface } \beta\text{)}. \tag{5.24}$$

The r.h.s. of (5.23) is zero for the cases of completely coherent reflexion ($S \ll \frac{1}{8}\lambda$) and completely incoherent reflexion ($S \gg \frac{1}{8}\lambda$) and reaches a maximum value of

$$|\langle \rho^2 \exp\{2i\chi\} \rangle_\tau - \langle \rho \exp\{i\chi\} \rangle_\tau^2|_{\max} = a^2(\tau)/32h^2, \tag{5.25}$$

which occurs when

$$S = 0.07\lambda \quad \text{and} \quad L^2 \gg h\lambda/2\pi, \tag{5.26}$$

corresponding to a rather particular gently undulating surface of very low relief. The upper bound (5.25) is likely to occur only infrequently and is in any case rather small, so that no serious approximation (and certainly no qualitative error of interpretation) arises if (5.22) is taken as being true in all cases.

Having demonstrated the applicability of all the statistical equations (4.17) to (4.40), we now write down the two basic quantities involved in them. The first is the *variance* Σ of ξ or η; from (4.18*a*), (4.19) and (5.20) (with $R = 0$), we have (writing the τ-dependence explicitly)

$$\Sigma(\tau) = \frac{1}{2}\int_0^\infty d\tau' Q(\omega_0^2, \tau') \left[\frac{\langle a^2(\tau - \tau' + (2f/c)) \rangle}{4h^2} - |\langle \rho \exp\{i\chi\} \rangle_{\tau-\tau'}|^2\right], \tag{5.27}$$

where $\langle \rho \exp\{i\chi\}\rangle_\tau$ is given by (5.5). The second is the *autocorrelation function* $C_{\psi_c\psi_c^*}(R)$ of ξ or η; from (4.1), (4.18b) and (5.20) we have

$$C_{\psi_c\psi_c^*}(R) = C_\psi(\tau, R) = \frac{\int_0^\infty d\tau' Q(\omega_0^2, \tau')\, J_0\left(2R\omega_0\sqrt{\frac{\tau'}{ch}}\right)\left[\frac{\langle a^2(\tau-\tau'+(2f/c)\rangle}{4h^2} - |\langle \rho \exp\{i\chi\}\rangle_{\tau-\tau'}|^2\right]}{2\Sigma(\tau)}. \tag{5.28}$$

Finally, we write the corresponding equations for the surface γ, which can be derived in a straightforward manner by the methods used throughout this section:

$$\Sigma(\tau) = \tfrac{1}{2}[\langle Z^2\rangle - \langle Z\rangle^2]\int_0^\infty d\tau' Q_Z(\tau')\frac{a^2(\tau-\tau')}{4h^2}, \tag{5.29}$$

$$C_{\psi_c\psi^*}(R) = C_\psi(\tau, R) = \frac{\int_0^\infty d\tau' Q_Z(\tau')\, J_0\left(2R\omega_0\sqrt{\frac{\tau'}{ch}}\right) a^2(\tau-\tau')}{\int_0^\infty d\tau' Q_Z(\tau')\, a^2(\tau-\tau')}, \tag{5.30}$$

where
$$Q_Z(\tau') = \frac{L^2\omega_0^2}{ch}\exp\{-\omega_0^2 L^2\tau'/ch\} \quad \text{(autocorrelation model 3.20)}, \tag{5.31}$$

$$= \frac{1}{2}\left(\frac{ch}{4\omega_0^2L^2}\right)^{\frac{1}{2}}\left(\tau' + \frac{ch}{4\omega_0^2L^2}\right)^{-\frac{3}{2}} \quad \text{(autocorrelation model 3.28)}. \tag{5.32}$$

These results for the three types of surface can be written in a unified form for the commonly-occurring case where $S \lesssim \sigma$. We define a 'coherence parameter'

$$\delta \equiv \exp\{-16\pi^2S^2/\lambda^2\} \quad \text{(surfaces } \alpha, \beta), \tag{5.33}$$

$$\equiv \langle Z\rangle^2/\langle Z^2\rangle \quad \text{(surface } \gamma), \tag{5.34}$$

whose value lies between 0 (complete incoherence) and 1 (complete coherence). We define also

$$Q(\tau') = Q(\omega_0^2, \tau') \quad \text{(surfaces } \alpha, \beta), \tag{5.35}$$

$$= Q_Z(\tau') \quad \text{(surface } \gamma), \tag{5.36}$$

so that $Q(\tau')$ is a monotonically decreasing function of positive τ' whose form depends on the rough surface and whose integral (from 5.17) is unity.

Then (5.27) to (5.30) become

$$\Sigma(\tau) \overset{(s<\sigma)}{=} \frac{\langle Z^2\rangle}{8h^2}(1-\delta)\int_0^\infty d\tau' Q(\tau')\, a^2(\tau-\tau'), \tag{5.37}$$

$$C_\psi(\tau, R) \overset{(s<\sigma)}{=} \frac{\int_0^\infty d\tau' Q(\tau')\, J_0(2R\omega_0\sqrt{(\tau'/ch)})\, a^2(\tau-\tau')}{\int_0^\infty d\tau' Q(\tau')\, a^2(\tau-\tau')}. \tag{5.38}$$

6. The average echo power

This is $\langle\psi^2(\tau, \boldsymbol{R}_0)\rangle$ which from (4.7) is given by the sum of its coherent and incoherent parts

$$\langle\psi^2(\tau, \boldsymbol{R}_0)\rangle = \langle\psi(\tau, \boldsymbol{R}_0)\rangle^2 + \Sigma(\tau), \tag{6.1}$$

where $\langle\psi(\tau, \boldsymbol{R}_0)\rangle$ is given by (5.6) and $\Sigma(\tau)$ by (5.27) or (5.29). The average value of the *smoothed* echo power is given by (2.19) and (4.19) as

$$\langle(\psi^2(\tau, \boldsymbol{R}_0))_{\mathrm{sm}}\rangle = \tfrac{1}{2}\langle\rho^2\rangle_\tau = \tfrac{1}{2}|\langle\psi_{\mathrm{c}}(\tau, \boldsymbol{R}_0)\rangle|^2 + \Sigma(\tau), \tag{6.2}$$

where $\langle\psi_{\mathrm{c}}(\tau, \boldsymbol{R}_0)\rangle$ is given by (5.1) and (5.5). The order of the operations of time-smoothing and ensemble averaging is immaterial, since it is obvious from (6.1) and (6.2) that

$$\langle\psi^2(\tau, \boldsymbol{R}_0)\rangle_{\mathrm{sm}} = \langle(\psi^2(\tau, \boldsymbol{R}_0))_{\mathrm{sm}}\rangle. \tag{6.3}$$

In the following nine subsections we shall explore the physical content of equations (6.1) and (6.2).

6 (i). *Total energy in the echo*

The arguments of this section are restricted to the rough surfaces α and β, for which the reflectivity $Z(\boldsymbol{R})$ is unity. The total energy E is defined as

$$E \equiv \int_{-\infty}^{\infty} \mathrm{d}\tau\langle\psi^2(\tau, \boldsymbol{R}_0)\rangle. \tag{6.4}$$

By applying the methods of § 5 (ii) to (2.12), it can be shown that

$$E = \frac{1}{4h^2}\int_{-\infty}^{\infty} \mathrm{d}\tau F^2(\tau) \tag{6.5}$$

exactly. Thus, within the Fresnel approximation, the energy received back from a totally reflecting rough surface of arbitrary form, with pulses which need not be quasimonochromatic, is, on average, the same as would return from a flat mirror – a result which is almost obvious. The minor approximations introduced towards the end of § 5 (ii) mean that (6.5) does not hold exactly for our calculated echo power (6.1); but the error is of order $\exp\{-2\pi^2\sigma^2/\lambda^2\}$ which can certainly be neglected in view of (1.1).

6 (ii). *The form of the echo tail*

The most obvious property of $\langle\psi^2(\tau, \boldsymbol{R}_0)\rangle$ is the asymmetrical lengthening of the pulse to include long positive delay times τ; this effect, produced by the integrals over τ' in the expressions (5.27) and (5.29) for $\Sigma(\tau)$ contrasts with the behaviour of $\langle\psi(\tau, \boldsymbol{R}_0)\rangle$, whose duration is, from (5.6), the same as that of the original pulse, i.e. σ/c. For the average echo power, therefore (either smoothed or not smoothed), we require the asymptotic form of $\Sigma(\tau)$ when $\tau \gg \sigma/2c$. The functions $\langle a^2(\tau - \tau' + (2f/c))\rangle$, $\langle\rho\exp\{\mathrm{i}\chi\}\rangle_{\tau-\tau'}$ and $a^2(\tau - \tau')$ in (5.27) and (5.29) are all localized near $\tau' = \tau$ because of the finite duration σ/c of the pulse $F(t)$, and $Q(\omega_0^2, \tau')$ and $Q_Z(\tau')$ may be treated as constant for this range of values of τ', and taken outside the integrals for $\Sigma(\tau)$. Making use of (5.5) and (6.5), the results given by this procedure are

$$\Sigma(\tau) \xrightarrow{\tau \gg \sigma/2c} Q(\omega_0^2, \tau)\, E(1 - \exp\{-16\pi^2 S^2/\lambda^2\}) \quad \text{(surfaces } \alpha, \beta), \tag{6.6}$$

$$\xrightarrow{\tau \gg \sigma/2c} Q_Z(\tau)\, E(\langle Z^2\rangle - \langle Z\rangle^2) \quad \text{(surface } \gamma). \tag{6.7}$$

If the surface relief is extremely low, and the reflectivity almost constant, the factors in ( ) vanish in (6.6) and (6.7) and the echo tail $\Sigma(\tau)$ is of zero strength, as would be expected in this case, which corresponds to a completely coherent echo. Any echo for which an appreciable tail is observed may safely be considered as completely incoherent, since the transition between

coherence and incoherence takes place within a narrow range of values of S centred on $\frac{1}{8}\lambda$. The manner in which the echo decays to zero with increasing τ depends on the functions $Q(\omega_0^2, \tau)$ and $Q_Z(\tau)$. These are given by (5.15), (5.16), (5.31) and (5.32) for exponential and Gaussian autocorrelation functions defined in §3. For general autocorrelation functions, the Q-functions are given by the Bessel transforms

$$Q(\omega_0^2, \tau) = \frac{2\omega_0^2}{ch}\int_0^\infty \mathrm{d}R\, R J_0\left(2R\omega_0\sqrt{\frac{\tau}{ch}}\right) C_f\left(\frac{2S\omega_0 R}{c\sqrt{(1-\exp\{-4S^2\omega_0^2/c^2\})}}\right) \quad \text{(surface } \alpha\text{)}, \tag{6.8}$$

$$= \frac{2\omega_0^2}{ch}\int_0^\infty \mathrm{d}R\, R J_0\left(2R\omega_0\sqrt{\frac{\tau}{ch}}\right) C_f(R) \quad \text{(surface } \beta\text{)}, \tag{6.9}$$

$$Q_Z(\tau) = \frac{2\omega_0^2}{ch}\int_0^\infty \mathrm{d}R\, R J_0\left(2R\omega_0\sqrt{\frac{\tau}{ch}}\right) C_Z(R) \quad \text{(surface } \gamma\text{)}, \tag{6.10}$$

where a simple generalization of the substitution (3.23) has been used in arriving at (6.8). These equations can easily be inverted to obtain the surface autocorrelation function $C_f(R)$ or $C_Z(R)$ from measurements of the echo tail $\Sigma(\tau)$, provided the nature of the surface is known. This type of inference will be discussed in §6 (ix).

6 (iii). *Duration of the echo*

We define the *echo half-length* T as the time measured from $\tau = 0$ (i.e. $t = 2h/c$) which must elapse on average before half the total received energy has arrived back at the source; thus (cf. 6.4)

$$\int_{-\infty}^{T} \mathrm{d}\tau \langle \psi^2(\tau, \boldsymbol{R}_0)\rangle \equiv \tfrac{1}{2}E. \tag{6.11}$$

The exact expression for T is rather complicated, and we shall content ourselves with a good approximation (exact when the echo is perfectly coherent or perfectly incoherent), which consists simply in taking the mean of the separate half-lengths of the coherent and incoherent parts of the echo, weighted according to their relative strengths. The coherent contribution $\langle \psi(\tau, \boldsymbol{R}_0)\rangle^2$ has a half-length of zero (i.e. half of it has arrived by the instant $\tau = 0$) and a strength

$$\exp\{-16\pi^2 S^2/\lambda^2\}$$

(cf. 5.6) for surfaces α and β and $\langle Z\rangle^2$ for surface γ. The incoherent contribution $\Sigma(\tau)$ has a half-length T_Σ given very accurately (cf. 5.27) and (5.29) by

$$\int_0^{T_\Sigma} Q(\tau)\, \mathrm{d}\tau = \tfrac{1}{2}, \tag{6.12}$$

where $Q(\tau)$ denotes $Q(\omega_0^2, \tau)$ or $Q_Z(\tau)$, and a relative strength given by $1-\delta$ for the rough surfaces α and β and $\langle Z^2\rangle(1-\delta)$ for the flat surface γ. Thus the approximate echo half-length is

$$T = T_\Sigma(1-\delta) \tag{6.13}$$

for all surfaces, where δ is given by (5.33) and (5.34).

The quantity T_Σ can easily be calculated from (6.12) to give the following final expressions for the echo half-lengths:

$$T = 2.77hS^2/cL^2 \quad \text{(surface } \alpha\text{)}, \tag{6.14}$$

$$= \frac{3h\lambda^2}{16\pi^2 cL^2}(1-\delta) \quad \text{(surfaces } \beta, \gamma\text{)}. \tag{6.15}$$

(In fact the half-length for surface γ depends to a small extent on whether the surface auto-correlation function (3.20) or (3.28) is used, but this only affects the numerical factor in (6.15) by a small percentage.)

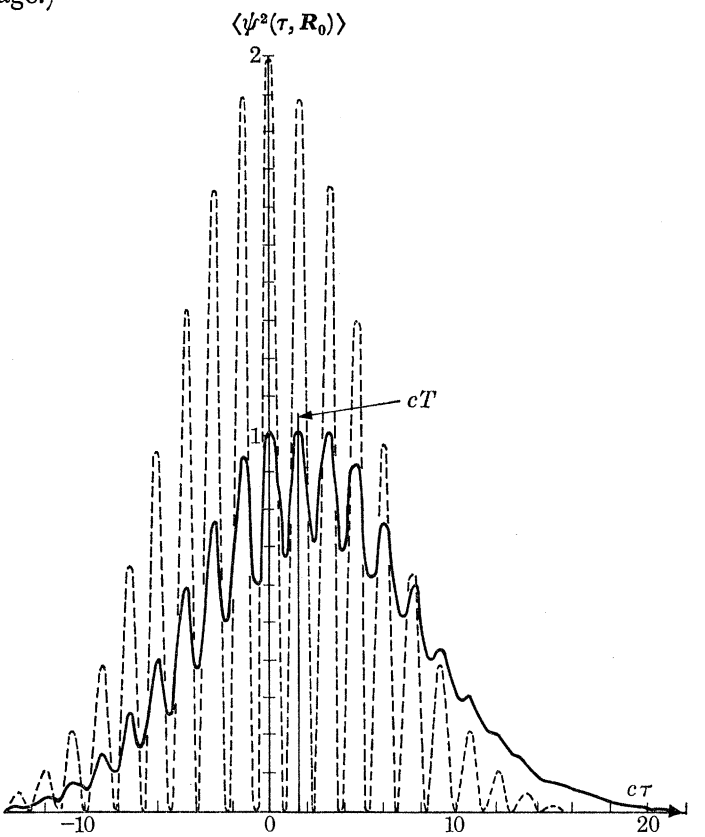

FIGURE 3. ———, Computer calculation of average echo power for long-wave case (undulating rough surface α, $\lambda = 3$, $\sigma = 10$, $h = 100$, $S = 0.3$, $L = 4$, r.m.s. surface slope = 6.07°, half-power time $T = 1.56/c$); – – – –, echo from flat mirror surface.

The evaluation of T provides a useful test of the applicability of the Fresnel approximation to Kirchhoff's integral introduced in §2(i). In order for our treatment to give a quantitatively accurate description of the bulk of the echo power, T must be sufficiently small that $\theta(\tau)$ (equation (2.17)) does not exceed about 45° (equation (2.10)). Thus we require that

$$T < 0.83h/c. \tag{6.16}$$

In the case of the undulating surface α, this condition may be expressed with the aid of (6.14) and (3.22) as

$$\langle f'^2\rangle < 0.6, \tag{6.17}$$

where $\langle f'^2\rangle$ is the mean square surface gradient; thus the average surface slopes should not exceed about 40°. This result has an obvious interpretation in geometrical optics (see §6(viii) below). For the surfaces β and γ the applicability condition (6.15) implies

$$\lambda/L < 6.6, \tag{6.18}$$

where we have simplified to the case of complete incoherence. The physical interpretation of (6.18) is that the Fraunhofer diffraction pattern of radiation from a horizontal irregularity of size $4L$ (cf. 3.29), illuminated at an angle of 45° to the vertical, is insufficiently wide to reflect significantly back to the source.

6 (iv). *Long-wave limit*

In this case λ so greatly exceeds the height S of surfaces α and β that the irregularities are not perceived by the exploring pulse, which is reflected as from a perfect mirror. The condition for this is

$$\lambda \gg 4\pi S, \tag{6.19}$$

which does not involve L (cf. 5.33). When this condition is satisfied, the variance $\Sigma(\tau)$ vanishes, due to the cancellation of the two terms in [ ] in (5.27), and the echo is completely coherent, the power being given by $\langle\psi(\tau, \boldsymbol{R}_0)\rangle^2$ (cf. (6.1)) which in this case takes the 'perfect-mirror' form

$$\langle\psi^2(\tau, \boldsymbol{R}_0)\rangle \xrightarrow{\text{long wave}} \frac{F(\tau)^2}{4h^2} \tag{6.20}$$

(cf. (2.13)). According to (6.19), however, this limit is only reached for very smooth surfaces – the pulse 'picks up' any irregularities whose r.m.s. height exceeds about 0.1λ, as illustrated by the partial quenching of the oscillatory part of the echo in figure 3.

For the flat surface γ the long-wave limit is identical with the Fraunhofer limit which will be treated in § 6 (vi).

6 (v). *Smooth-surface limit*

This occurs when the horizontal dimension L of the irregularities is large. The precise conditions are

$$L \gg 2S\sqrt{\frac{h}{\sigma(1-\exp\{-16\pi^2S^2/\lambda^2\}}} \quad \text{(surface } \alpha\text{)}, \tag{6.21}$$

$$L \gg \frac{\lambda}{2\pi}\sqrt{\frac{h}{\sigma}} \quad \text{(surfaces } \beta, \gamma\text{)}, \tag{6.22}$$

which enable $Q(\omega_0^2, \tau)$ and $Q_Z(\tau)$ (equations (5.15), (5.16), (5.31) and (5.32)) to be replaced by

$$Q_Z(\tau) = Q(\omega_0^2, \tau) \to \delta(\tau) \tag{6.23}$$

in the integrals (5.27) and (5.29), so that the variance becomes

$$\Sigma(\tau) \to \frac{1}{2}\left[\frac{\langle a^2(\tau+(2f/c)\rangle}{4h^2} - |\langle\rho\exp\{\mathrm{i}\chi\}\rangle_\tau|^2\right] \quad \text{(surfaces } \alpha, \beta\text{)}, \tag{6.24}$$

$$\to \tfrac{1}{2}[\langle Z^2\rangle - \langle Z\rangle^2]\frac{a^2(\tau)}{4h^2} \quad \text{(surface } \gamma\text{)}, \tag{6.25}$$

where $\langle a^2(\tau+(2f/c))\rangle$ is given by (5.21). Using (6.1), (5.6) and (5.9), we obtain, for the mean echo power:

$$\langle\psi^2(\tau, \boldsymbol{R}_0)\rangle \xrightarrow{L\to\infty} \frac{1}{2.4h^2}\left\{\left\langle a^2\left(\tau+\frac{2f}{c}\right)\right\rangle + \exp\left\{-\frac{16\pi^2S^2}{\lambda^2}\right\}a^2(\tau)\cos 2\omega_0\tau\right\} \quad \text{(surfaces } \alpha, \beta\text{)}, \tag{6.26}$$

$$\xrightarrow{L\to\infty} \frac{a^2(\tau)}{2.4h^2}\{\langle Z^2\rangle + \langle Z\rangle^2\cos 2\omega_0\tau\} \quad \text{(surface } \gamma\text{)}. \tag{6.27}$$

Actually, these expressions are not quite accurate; the factor $\exp\{-16\pi^2S^2/\lambda^2\}$ in (6.28) should be replaced by $\exp\{-32\pi^2S^2/\lambda^2\}$, and the factor $\langle Z\rangle^2$ in (6.27) by $\langle Z^2\rangle$. The errors arise from the statistical assumptions (4.17) and (4.18*a*) (it is not surprising that these assumptions may break down in this case, where the surface is flat and has constant reflectivity, over the

'neighbourhood' seen by the source-receiver). The errors are, however, rather small (cf. the discussion after (5.24)), and do not affect the average time-smoothed power $\langle(\psi^2(\tau, \boldsymbol{R}_0))_{\mathrm{sm}}\rangle$ which is obtained from (6.26) and (6.27) simply by setting the oscillatory factors $\cos 2\omega_0\tau$ equal to their mean value of zero. It is possible to evaluate the smooth-surface limit exactly by averaging the square of (2.12) directly, setting the surface autocorrelation functions $C_f(\boldsymbol{R})$ and $C_Z(\boldsymbol{R})$ equal to unity. The results are

$$\langle\psi^2(\tau, \boldsymbol{R}_0)\rangle \xrightarrow{L\to\infty} \frac{\langle F^2(\tau+(2f/c))\rangle}{4h^2} \equiv \frac{1}{4h^2}\int_{-\infty}^{\infty} \mathrm{d}f P_1^f(f)\, F^2(\tau+(2f/c)) \quad \text{(surfaces } \alpha, \beta\text{)}, \tag{6.28}$$

$$\langle\psi^2(\tau, \boldsymbol{R}_0)\rangle \xrightarrow{L\to\infty} \frac{\langle Z^2\rangle}{4h^2} F^2(\tau) \quad \text{(surface } \gamma\text{)}, \tag{6.29}$$

which can easily be seen to differ from (6.26) and (6.27) in the manner stated, and to have the simple physical interpretation that in this limit the echo power is reflected as from an ensemble of mirrors whose heights and reflectivities are individually constant, but differ from different members of the ensemble. Since both terms in (6.1) may contribute to the echo, it is neither completely coherent nor completely incoherent in this case.

6 (vi). *Fraunhofer limit*

This is the opposite case to the smooth-surface limit: the source-receiver is so far above the surface, or the irregularities so small, that the exploring pulse perceives the surface as 'completely rough' (this is the situation encountered in pulse echo investigations of the Moon and planets – see Beckmann & Spizzichino 1963, ch. 20). When the conditions

$$h \gg \frac{L^2\sigma}{4S^2}\left(1-\exp\{-16\pi^2S^2/\lambda^2\}\right) \quad \text{(surface } \alpha\text{)}, \tag{6.30}$$

$$h \gg \frac{4\pi^2L^2\sigma}{\lambda^2} \quad \text{(surfaces } \beta, \gamma\text{)} \tag{6.31}$$

are satisfied (which are much more restrictive than (4.2) which merely guarantees that the echo statistics are Gaussian), the functions $Q(\omega_0^2, \tau')$ and $Q_Z(\tau')$ are very small, so that the incoherent component $\Sigma(\tau)$ of the echo power is very small ((5.27), (5.29)). Thus, from (6.1), the echo power is given by the short-lived coherent component alone:

$$\langle\psi^2(\tau, \boldsymbol{R}_0)\rangle \xrightarrow{\text{Fraunhofer limit}} \langle\psi(\tau, \boldsymbol{R}_0)\rangle^2, \tag{6.32}$$

where $\langle\psi(\tau, \boldsymbol{R}_0)\rangle$ is given by (5.6) or (5.9).

It looks at first sight as though in the Fraunhofer limit the echo violates the total-energy equation (6.5), because

$$\int_{-\infty}^{\infty} \mathrm{d}\tau\langle\psi^2(\tau, \boldsymbol{R}_0)\rangle = \frac{\exp\{-16\pi^2S^2/\lambda^2\}}{4h^2}\int_{-\infty}^{\infty} \mathrm{d}\tau F^2(\tau). \tag{6.33}$$

But this is not the case, because the incoherent component $\Sigma(\tau)$ of the power, whose magnitude is very small, has a very long duration T_Σ (cf. (6.14), (6.15)), so that the echo has a long weak tail, which can easily be shown to contain the missing energy. This is illustrated by the computer calculation of figure 4.

6 (vii). *Continuous wave limit*

This is the case where the original pulse is monochromatic, so that the pulse-length σ is infinite, and (cf. (2.2), (2.4)) we may take

$$F(t) = A\cos\omega_0 t. \tag{6.34}$$

The variance $\Sigma(\tau)$ is easily calculated using the property (5.17), leading to the result

$$\langle\psi^2(\tau, \boldsymbol{R}_0)\rangle \xrightarrow{\sigma\to\infty} \frac{A^2\langle Z^2\rangle}{2.4h^2}(1+\delta\cos 2\omega_0\tau) \tag{6.35}$$

which applies to all three surfaces. This expression closely resembles the 'smooth-surface' results (6.26) and (6.27), and, indeed, requires the conditions (6.21) and (6.22) to hold for its validity.

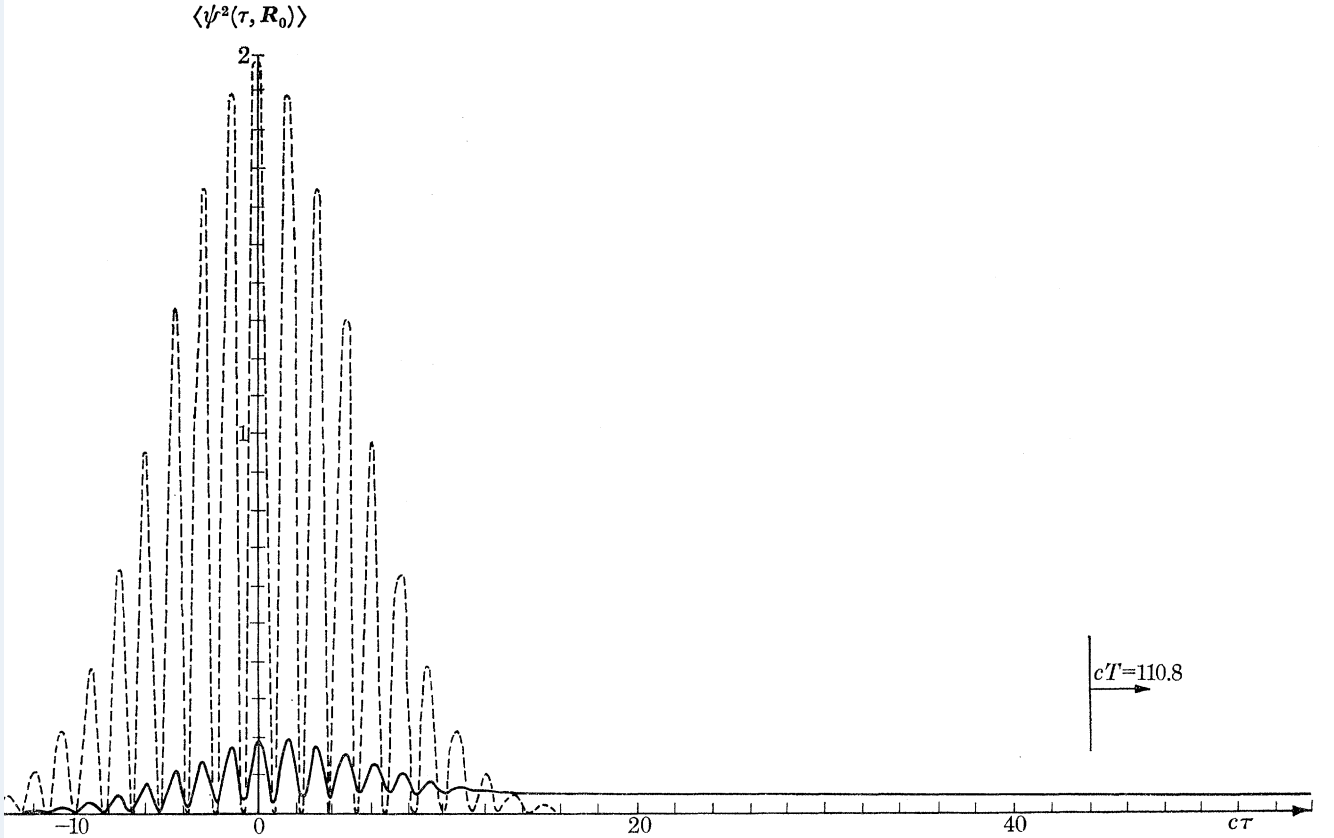

FIGURE 4. ———, Computer calculation of average echo power for Fraunhofer case (undulating rough surface α, $\lambda = 3$, $\sigma = 10$, $h = 1000$, $S = 0.375$, $L = 1.875$, r.m.s. surface slope = 16.2°, half-power time $T = 110.8/c$); – – – –, echo from flat mirror surface.

6 (viii). *Geometrical-optics limit*

In this case, which is the opposite situation to the long-wave limit treated in § 6 (iv), the wavelength is so short that for the surfaces α and β all oscillatory effects are washed out by phase averaging, and the echo power is the same as would be received if a burst of *particles* were emitted from the source with time-dependence $\frac{1}{2}a^2(t)$, and reflected specularly from the rough surface. This requires the condition

$$\lambda \ll 4\pi S, \tag{6.36}$$

which causes the coherent term $\langle\psi(\tau, \boldsymbol{R}_0)\rangle^2$ in (6.1) to vanish in view of (5.6), and the second term $|\langle\rho\exp\{i\chi\}\rangle|^2$ in (5.27) to vanish in view of (5.5). Thus the echo is purely incoherent in this limit, as illustrated in figure 5.

For the undulating rough surface α, the geometrical-optical average echo power is, using (5.15),

$$\langle\psi^2(\tau, \boldsymbol{R}_0)\rangle \xrightarrow[\text{optics}]{\text{geometrical}} \frac{1}{2.4h^2}\frac{cL^2}{4S^2h}\int_0^\infty d\tau' \exp\left\{-\frac{cL^2\tau'}{4S^2h}\right\}\langle a^2(\tau-\tau'+(2f/c))\rangle. \tag{6.37}$$

The physical meaning of this expression is that for each time delay τ there are contributions to the echo from a small range of time delays τ' (the duration of the range being roughly σ/c), resulting from specular reflexion from parts of the surface inclined to the horizontal at an angle $\theta(\tau')$ given by (2.17) (see figure 2). The surface slopes $f' \approx \theta(\tau')$ possess the Gaussian probability distribution $\Pi(f')$ given by (3.22), whose exponential factor,

$$\exp\{-L^2 f'^2/4S^2\} = \exp\{-cL^2\tau'/4hS^2\}, \tag{6.38}$$

is exactly what appears in (6.37), expressing the improbability of finding slopes on the surface sufficiently steep to return echoes after long time delays.

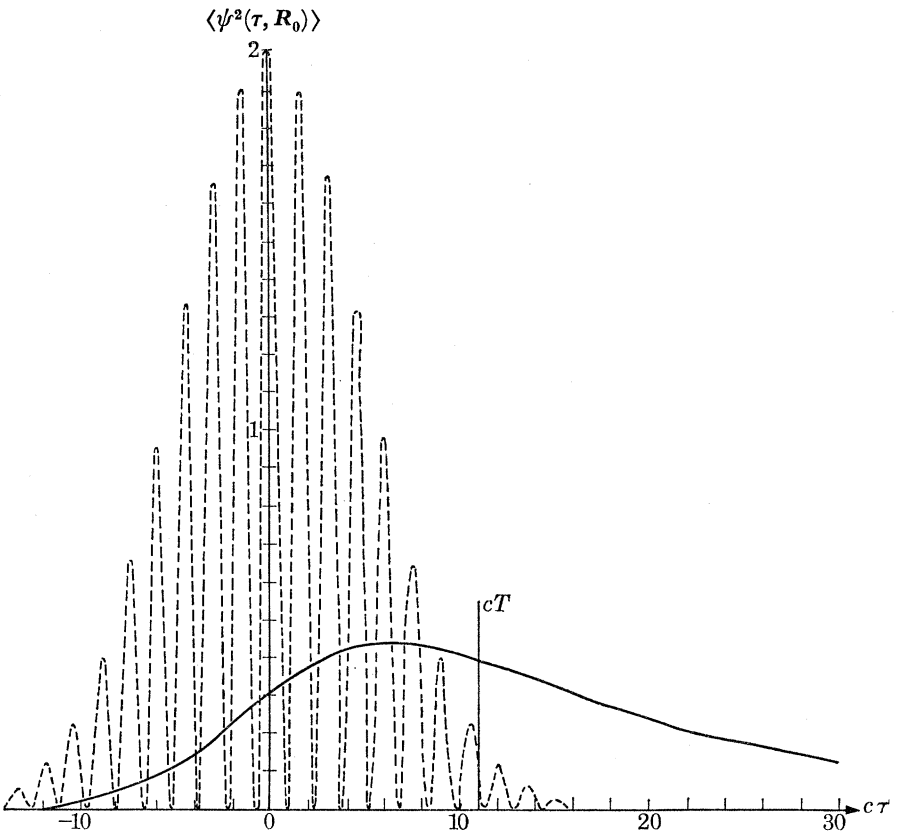

FIGURE 5. ———, Computer calculation of average echo power for geometrical optics case (undulating rough surface α, $\lambda = 3$, $\sigma = 10$, $h = 100$, $S = 3$, $L = 15$, r.m.s. surface slope = 16.2°, half-power time $T = 11.1/c$).

For the stepped surface β, the geometrical-optical average power is, using (5.16),

$$\langle\psi^2(\tau, R_0)\rangle \xrightarrow{\text{geometrical optics}} \frac{1}{2.4h^2}\left\langle a^2\left(\tau + \frac{2f}{c}\right)\right\rangle, \tag{6.39}$$

expressing the fact that only those steps immediately below the source-receiver are capable of specular back-reflexion. This result is the incoherent ($\lambda \to 0$) limit of the smooth-surface expression (6.26).

For the flat surface γ the geometrical-optics limit is identical with the smooth-surface limit (6.27).

6 (ix). *Inferences about the surface from the average echo power*

We are concerned in this section with what is theoretically possible, not what is practicable (this will in any case depend on the particular experimental situation). If the nature of the

surface is known *a priori*, then it is not too hard to obtain information about the surface parameters, by measuring the echo half-length T. For instance, suppose the surface is known to be of the undulating 'Gaussian' type α, considered in §3 (i); then the r.m.s. slope $\sqrt{2}\,S/L$ can be inferred directly from a measurement of T by using (6.14). In the general case, where nothing is known *a priori* about the surface, the problem is more difficult; to simplify it, we assume that the surface is one of the three types introduced in §3. These surfaces are physically very different, so that this procedure does take some account of the enormous diversity of natural rough surfaces.

The first step is to discover δ, the degree of coherence of the echo, defined by (5.33 and 5.34). This is most easily done with continuous waves (§6 (vii)), by measuring the *unsmoothed* ensemble average $\langle\psi^2(\tau, \boldsymbol{R}_0)\rangle$ in the 'neighbourhood' under investigation. According to equation (6.35), this quantity is the sum of an oscillatory term and a steady term, the ratio of whose strength is simply δ. This ratio can be measured; if its value is close to unity, then the reflexion is coherent, and all that can be inferred about the surface is that it is flat on a wavelength scale, with a reflectivity which hardly varies with position. If δ is less than unity, then the surface roughness is appreciable. To distinguish the undulating (α) and stepped (β) surfaces from the surface of varying reflectivity (γ) it is merely necessary to alter the wavelength and observe the effect of this on the ratio of the oscillatory to the steady parts of the echo; if the δ decreases as λ decreases, then we know that we are looking at either an undulating or a stepped surface, and the r.m.s. height S can be inferred from (6.35), while if δ does not alter as λ varies, then we know that the surface is flat, and the ratio $\langle Z\rangle^2/\langle Z^2\rangle$ can be inferred from (6.35) (we assume that $Z(\boldsymbol{R})$ does not vary significantly with λ in the range of interest).

Armed with this information, the next step is to use a finite pulse length σ, measure the echo half length T, and use equations (6.14, 6.15) to infer L. If the surface has been found to be flat, then (6.15) can be employed directly to find L, since $\langle Z\rangle^2/\langle Z^2\rangle$ has already been found, and h is known from the time delay of the echo as a whole. To distinguish undulating and stepped surfaces, the wavelength dependence of T is investigated. If T is constant as λ varies then the surface is undulating, and L can be calculated from (6.14). If T varies with λ, then the surface is stepped, and L can be calculated from (6.15).

The final step is to infer the surface autocorrelation function $C_f(\boldsymbol{R})$ or $C_Z(\boldsymbol{R})$ from the form of the incoherent tail of $\langle\psi^2(\tau, \boldsymbol{R}_0)\rangle$ which according to §6 (ii) is proportional to $Q(\tau)$.

Equations (6.8) to (6.10) can be inverted, to give

$$\left.\begin{aligned}\int_0^\infty \mathrm{d}\tau\, Q(\tau)\, J_0\left(2R\omega_0\sqrt{\frac{\tau}{ch}}\right) &= C_f\left(\frac{RS\omega_0}{c\sqrt{(1-\exp\{-S^2\omega_0^2/c^2\})}}\right) \quad \text{(surface } \alpha\text{)},\\ &= C_f(R) \quad \text{(surface } \beta\text{)},\\ &= C_Z(R) \quad \text{(surface } \gamma\text{)}.\end{aligned}\right\} \tag{6.40}$$

This method may enable $C(R)$ to be determined for small or moderate R, since the integral in (6.40) then depends on $Q(\tau)$ for large τ but will fail at large R, since the integral then depends on $Q(\tau)$ for small τ – i.e. not on the tail at all.

Thus it is possible, at least in principle, to employ measurements of the average echo power $\langle\psi^2(\tau, \boldsymbol{R}_0)\rangle$ to infer the nature of the rough surface, the parameters L and S or $\langle Z\rangle^2/\langle Z^2\rangle$, and the autocorrelation function $C_f(R)$ or $C_Z(R)$, i.e. all the statistical quantities introduced in §3. No information about the surface can be obtained from the statistics of the spatial fading observed as the source-receiver position $\boldsymbol{R}_0$ is varied, but we shall see in §7 (ii) that this fading can provide a very sensitive method of defining position relative to the surface as a whole.

7. The spatial fading pattern

Spatial fading is the variation of the echo as the source-receiver is moved. We are concerned in this paper only with horizontal movement, where $\boldsymbol{R}_0$ varies and h is held fixed (as is the delay time τ). The discussion will be divided into two sections: the first (§7 (i)) will be concerned with the spatial frequency and spectral purity of the pseudo-periodicity observed in the fading, while the second (§7 (ii)) will be concerned with the sensitivity of the echo to small changes in $\boldsymbol{R}_0$.

7 (i). *Periodicity of the fading*

The simplest quantity characterizing the spatial quasiperiodicity of the echo is the average number of times N_ξ that the echo wavefunction $\psi(\tau, \boldsymbol{R}_0)$ passes through its mean value when the source-receiver is moved horizontally along unit length of a straight line, the time delay τ being held fixed. (For the incoherent scattering with which we shall be principally concerned in this section, the mean value of $\psi(\tau, \boldsymbol{R}_0)$ is zero.) Writing the τ-dependence of N_ξ explicitly, and using (4.9) together with (5.28) and (5.30), we obtain

$$N_\xi(\tau) = \frac{4}{\lambda}\left(\frac{c\bar{\tau}(\tau)}{2h}\right)^{\frac{1}{2}}, \tag{7.1}$$

where $\bar{\tau}(\tau)$ is a 'modified delay time' defined by

$$\bar{\tau}(\tau) \equiv \frac{\int_0^\infty \mathrm{d}\tau' \tau' Q(\omega_0^2, \tau') \left[\frac{\langle a^2(\tau-\tau'+(2f/c))\rangle}{4h^2} - |\langle \rho \exp\{\mathrm{i}\chi\}\rangle_{\tau-\tau'}|^2\right]}{\int_0^\infty \mathrm{d}\tau' Q(\omega_0^2, \tau') \left[\frac{\langle a^2(\tau-\tau'+(2f/c))\rangle}{4h^2} - |\langle \rho \exp\{\mathrm{i}\chi\}\rangle_{\tau-\tau'}|^2\right]} \quad \text{(surfaces } \alpha, \beta), \tag{7.2}$$

$$\bar{\tau}(\tau) \equiv \frac{\int_0^\infty \mathrm{d}\tau' \tau' Q_Z(\tau')\, a^2(\tau-\tau')}{\int_0^\infty \mathrm{d}\tau' Q_Z(\tau')\, a^2(\tau-\tau')} \quad \text{(surface } \gamma), \tag{7.3}$$

a quantity the significance of which will be discussed in a moment. It is simpler in practice to measure the fading frequency for the amplitude, N_ρ, as discussed at the beginning of §4 (ii). The fastest spatial fading occurs when the amplitude ρ crosses the datum level $\Sigma^{\frac{1}{2}}$ (4.39), and (4.40) and (4.9) show that

$$N_\rho^{\max}(\tau) = 1.52 N_\xi(\tau), \tag{7.4}$$

so that calculation of the quasiperiodicity of both ρ and ξ requires a knowledge of $\bar{\tau}(\tau)$.

For observations in the echo tail, i.e. when

$$\tau \gg \sigma/2c, \tag{7.5}$$

it is easily seen from the temporal localization of $a^2(\tau)$ and $\langle \rho \exp\{\mathrm{i}\chi\}\rangle_\tau$ that (7.2) and (7.3) simplify to

$$\bar{\tau}(\tau) \xrightarrow{\tau \gg \sigma/2c} \tau. \tag{7.6}$$

When τ is not large, it is generally necessary to evaluate the integrals in (7.2) and (7.3) without approximation, but in the important class of situations where the echo has a long tail, more precisely when

$$T \gg \sigma/2c, \tag{7.7}$$

analysis of the integrals defining $\bar{\tau}(\tau)$ shows that the following approximation holds:

$$\bar{\tau}(\tau) = \frac{\int_0^\infty \mathrm{d}\tau' \tau' a^2(\tau - \tau')}{\int_0^\infty \mathrm{d}\tau' a^2(\tau - \tau')}. \tag{7.8}$$

This expression is independent of the form of the surface, and involves only the form of the pulse envelope $a(t)$. By using the model (2.4), $\bar{\tau}(\tau)$ can be evaluated in terms of the complementary error function; the result is

$$\bar{\tau}(\tau) = \frac{\sigma^2}{4c^2}\frac{\mathrm{d}}{\mathrm{d}\tau}\left[\ln\left(\exp\{2\tau^2c^2/\sigma^2\}\operatorname{erfc}\left(-\frac{\sqrt{2}\,c\tau}{\sigma}\right)\right)\right], \tag{7.9}$$

which has the limiting behaviour

$$\bar{\tau}(\tau) \begin{cases} \xrightarrow{\tau \gg \sigma/2C} \tau \\ \xrightarrow{\tau \simeq 0} 0.40\sigma/C \\ \xrightarrow{\tau \ll -\sigma/2C} \sigma^2/4C^2|\tau| \end{cases} \tag{7.10}$$

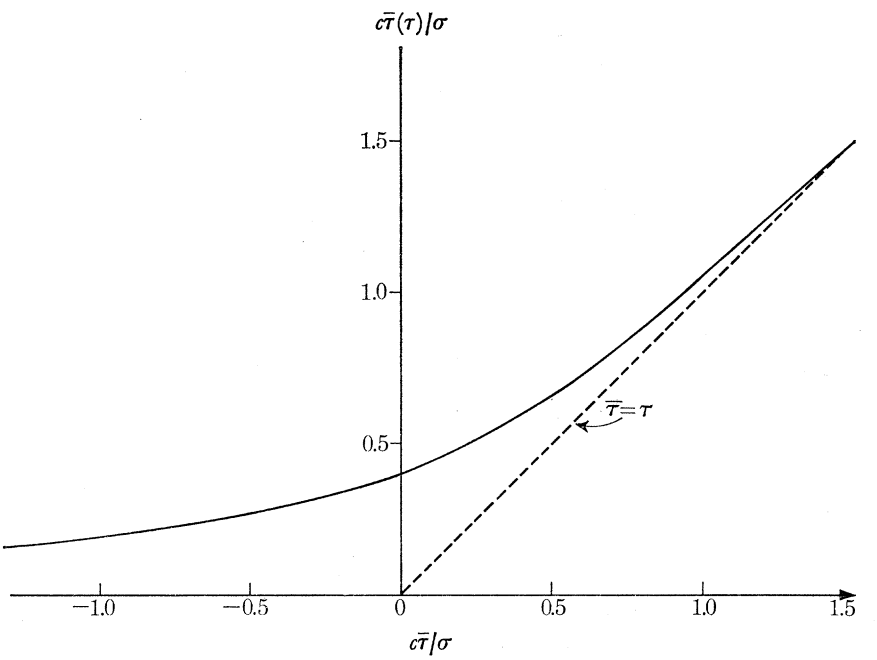

FIGURE 6. Modified delay time $\bar{\tau}(\tau)$ required to calculate the spatial fading frequency of the echo.

Figure 6 is a graph of the function $\bar{\tau}(\tau)$, which enables the fading frequency $N_\xi(\tau)$ or $N_\rho(\tau)$ to be predicted via (7.1) and (7.4) for any delay time τ, provided (7.7) holds. It is not expected that this procedure will always give quantitatively reliable results when τ is large and negative, because then the echo arises from the very early returns from isolated high points on the surface, and may not have the Gaussian distribution assumed in the derivation of (4.9).

The results (7.1) and (7.8) can be obtained from an elementary physical argument first given in outline by Robin *et al.* (1969). For a source-receiver position P_1, the echo at time delay τ comes from an annulus on the surface (figure 2), whose width is $\Delta R(\tau)$, given by (2.16). If the

source-receiver is displaced horizontally by $\Delta \boldsymbol{R}_0$, so that it now lies at P_2, then essentially the same region of the surface contributes to the echo, provided that

$$|\Delta \boldsymbol{R}_0| \ll \Delta R(\tau). \tag{7.11}$$

But the phase of the contribution from a point M on the annulus is different for the two source-receiver positions, because the path lengths $2P_1M$ and $2P_2M$ are different (figure 7). If M has an azimuth angle ϕ (measured from the direction of $\Delta \boldsymbol{R}_0$), then the change in path length is

$$2P_1M - 2P_2M = 2|\Delta \boldsymbol{R}_0| \sin\theta \cos\phi, \tag{7.12}$$

and the phase change $\Delta\chi$ in the contribution from M is

$$\Delta\chi = (4\pi/\lambda)\, |\Delta \boldsymbol{R}_0| \sin\theta \cos\phi. \tag{7.13}$$

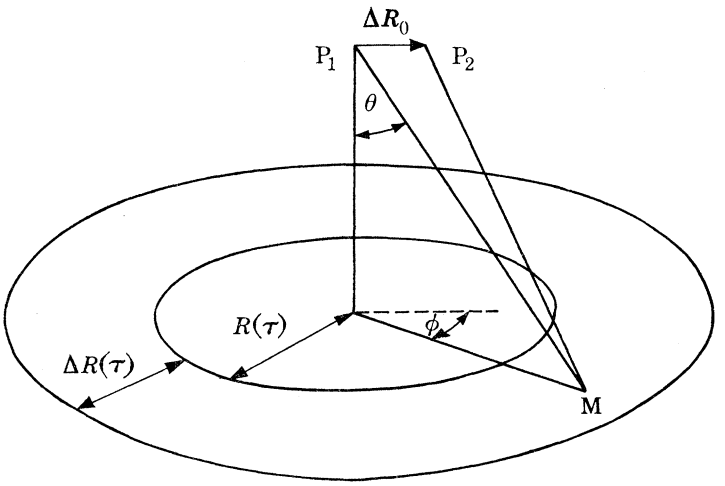

FIGURE 7. Path difference contributing to spatial fading.

The mean distance $|\Delta \boldsymbol{R}_0|_0$ between adjacent zeros of the echo wave function $\psi(\tau, \boldsymbol{R}_0)$ corresponds to a change of π in some *average value* of $\Delta\chi$ over the contributing annulus. If this average is taken as an r.m.s. value, then (7.13) gives

$$N_\xi(\tau) = \frac{1}{|\Delta \boldsymbol{R}_0|_0} = \frac{4}{\lambda}\sqrt{(\overline{\sin^2\theta \cos^2\phi})}. \tag{7.14}$$

To evaluate the annulus average $\overline{\sin^2\theta \cos^2\phi}$, we recall our assumption that the source radiation pattern is azimuthally symmetrical, and realize that the strength of the contribution from M will be proportional to the square of the pulse envelope, $a^2(\tau - \tau')$, where τ' is the time delay corresponding to θ (thus τ' labels the different rings in the annulus of figure 7). We have

$$\overline{\sin^2\theta \cos^2\phi} = \frac{\frac{1}{2}\int_0^\infty \mathrm{d}\tau' \sin^2\theta(\tau')\, a^2(\tau - \tau')}{\int_0^\infty \mathrm{d}\tau' a^2(\tau - \tau')}, \tag{7.15}$$

$$= \frac{c\bar{\tau}(\tau)\,(1 + c\bar{\tau}(\tau)/4h)}{2h(1 + (c\bar{\tau}(\tau)/2h))^2}, \tag{7.16}$$

where we have used (2.18), (7.8) and restricted ourselves to pulses for which $\sigma \ll h$. Substituting (7.16) into (7.14), we obtain

$$N_\xi(\tau) = \frac{4}{\lambda}\left(\frac{c\bar{\tau}(\tau)}{2h}\right)^{\frac{1}{2}} \frac{(1 + [c\bar{\tau}(\tau)/4h])^{\frac{1}{2}}}{1 + [c\bar{\tau}(\tau)/2h]}, \tag{7.17}$$

which, provided the condition (2.10) holds, reduces to the equation (7.1) derived from the more formal theory. Thus the fading is slowest near the first return, and reaches a maximum rate of $4/\lambda\sqrt{2}$ when $\tau\to\infty$ (this last result follows from (7.17) which holds even when (2.10) is violated).

Both the elementary and formal theories of the spatial fading frequency only hold if the mean distance $|\Delta\boldsymbol{R}_0|_0$ between zeros is smaller than the width $\Delta R(\tau)$ of the annulus of contributing points ((7.11) and (5.19)). This is always the case, however, since

$$\frac{|\Delta\boldsymbol{R}_0|_0}{\Delta R(\tau)}=\frac{1}{N_\xi(\tau)\,\Delta R(\tau)}\approx\frac{\lambda}{\sqrt{2}\,\sigma}, \tag{7.18}$$

which is small because of (1.1).

The formulae (7.1), (7.8) and (7.17) show that $N_\xi(\xi)$ is independent of the nature of the surface, which seems paradoxical, since no fading is observable for a flat perfect mirror surface. But our arguments have implied a large number of essentially independent scattering objects in the contributing annulus, so that the surface must satisfy the condition (4.2). Furthermore, the *visibility* of the fading predicted for a given time delay depends on the mean echo power

$$\langle\psi^2(\tau,\boldsymbol{R}_0)\rangle$$

being sufficiently large to be detected, and this certainly does involve the properties of the surface, as explained in §6. We shall return to this matter in §7 (ii).

Now we discuss the spectral purity of the spatial fading for fixed delay time, which can be characterized by $\epsilon(\tau)$, defined by

$$\epsilon(\tau)=\frac{\text{r.m.s. deviation of the distance between successive zeros from its mean value } |\Delta\boldsymbol{R}_0|_0}{|\Delta\boldsymbol{R}_0|_0}. \tag{7.19}$$

To calculate $\epsilon(\tau)$ we employ the methods introduced by Longuet-Higgins (1956) in an analysis of the statistics of random surfaces. We consider the echo $\psi(\tau,\boldsymbol{R}_0)$ to be a superposition of plane waves with (two-dimensional) wavenumbers $\boldsymbol{K}$ in the horizontal plane:

$$\psi(\tau,\boldsymbol{R}_0)=\iint\mathrm{d}\boldsymbol{K}[E(\boldsymbol{K},\tau)]^{\frac{1}{2}}\exp\{\mathrm{i}(\boldsymbol{K}\cdot\boldsymbol{R}_0+\chi(\boldsymbol{K},\tau))\}, \tag{7.20}$$

where the plane wave $\boldsymbol{K}$ has a phase $\chi(\boldsymbol{K},\tau)$ and an intensity $E(\boldsymbol{K},\tau)$. The function $E(\boldsymbol{K},\tau)$ is termed the 'power spectrum' of the echo; in the present problem the isotropy of the surface statistics demands that $E(\boldsymbol{K},\tau)$ is a function only of the length K of $\boldsymbol{K}$ (unlike the phase $\chi(\boldsymbol{K},\tau)$, which must depend on the direction of $\boldsymbol{K}$ if a particular source-receiver point $\boldsymbol{R}_0$ is not to be singled out). The echo autocorrelation function, $C_\psi(\tau,R)$ is the normalized Fourier transform of the power spectrum, which in this case may be written as

$$C_\psi(\tau,\boldsymbol{R})=\frac{\iint\mathrm{d}\boldsymbol{K}\,E(\boldsymbol{K},\tau)\exp\{\mathrm{i}\boldsymbol{K}\cdot\boldsymbol{R}\}}{\iint\mathrm{d}\boldsymbol{K}\,E(\boldsymbol{K},\tau)}, \tag{7.21}$$

$$=\frac{\int_0^\infty\mathrm{d}K\,KJ_0(KR)\,E(K,\tau)}{\int_0^\infty\mathrm{d}K\,KE(K,\tau)}. \tag{7.22}$$

The power spectrum is known, since our formulae (5.28) and (5.30) for $C_\psi(\tau,R)$ have the same form as (7.22) (i.e. they are Bessel transforms over R), with

$$K=2\omega_0(\tau'/ch)^{\frac{1}{2}}. \tag{7.23}$$

We are interested in the statistics of the fading as $\boldsymbol{R}_0$ varies along a straight line; thus we require a modified power spectrum $\mathscr{E}(q,\tau)$ (where q is again a wavenumber), defined by

$$C_\psi(\tau,R) = \frac{\int_0^\infty \mathrm{d}q \cos qR\,\mathscr{E}(q,\tau)}{\int_0^\infty \mathrm{d}q\,\mathscr{E}(q,\tau)}, \tag{7.24}$$

and

$$\mathscr{E}(q,\tau) = \int_q^\infty \mathrm{d}K \frac{KE(K,\tau)}{(K^2-q^2)^{\frac{1}{2}}}. \tag{7.24a}$$

The principal periodicity in $\psi(\tau,\boldsymbol{R}_0)$ encountered as the source moves along a line has a wavenumber equal to the r.m.s. value of q over the distribution $\mathscr{E}(q,\tau)$ (Longuet-Higgins 1956); from (7.24a), this is given by

$$\overline{q^2(\tau)} \equiv \frac{\int_0^\infty \mathrm{d}q\,q^2\mathscr{E}(q,\tau)}{\int_0^\infty \mathrm{d}q\,\mathscr{E}(q,\tau)} = \frac{\frac{1}{2}\int_0^\infty \mathrm{d}K\,K^3E(K,\tau)}{\int_0^\infty \mathrm{d}K\,KE(K,\tau)} = \tfrac{1}{2}\overline{K^2(\tau)}. \tag{7.25}$$

Our previously evaluated fading rate $N_\xi(\tau)$ is related to $\overline{q^2(\tau)}$ by

$$N_\xi(\tau) = \frac{(\overline{q^2(\tau)})^{\frac{1}{2}}}{\pi}, \tag{7.26}$$

and indeed a direct evaluation of $\overline{q^2(\tau)}$ by the use of (7.25) yields (7.1) exactly, which is a useful check. The factors of $\frac{1}{2}$ in (7.25) and (7.15) have the meaning: the fading rate is reduced by interference between points on the contributing annulus of figure 2 which lie far from the vertical plane through the direction of motion of the source-receiver, since the path-lengths to such points vary more slowly with $\boldsymbol{R}_0$ than the path-lengths to points lying fore-and-aft of the source.

We now have the machinery required to estimate the quantity $\epsilon(\tau)$ (7.19) which is a measure of the degree of periodicity of the fading. According to Rice (1945, § 3.4) and Longuet-Higgins (1956), $\epsilon(\tau)$ is approximately given by the r.m.s. width of the distribution $\mathscr{E}(q,\tau)$; the approximation is exact in the limit $\epsilon(\tau)\to 0$ – i.e. for a narrow power spectrum. From (7.24) we have

$$\epsilon(\tau) = \left[\frac{\int_0^\infty \mathrm{d}q(q-\bar{q})^2\mathscr{E}(q,\tau)}{\int_0^\infty \mathrm{d}q\,\mathscr{E}(q,\tau)}\right]^{\frac{1}{2}} = \left[1-\frac{8(\overline{K}(\tau))^2}{\pi^2\overline{K^2}(\tau)}\right]. \tag{7.27}$$

When the echo has a long tail, i.e. when (7.7) holds, it can be shown that

$$\epsilon(\tau) = \left[1-\frac{8(\overline{\tau^{\frac{1}{2}}}(\tau))^2}{\pi^2\overline{\tau}(\tau)}\right]^{\frac{1}{2}}, \tag{7.28}$$

where

$$\overline{\tau^{\frac{1}{2}}}(\tau) \equiv \frac{\int_0^\infty \mathrm{d}\tau'\tau'^{\frac{1}{2}}a^2(\tau-\tau')}{\int_0^\infty \mathrm{d}\tau' a^2(\tau-\tau')} \tag{7.29}$$

and $\overline{\tau}(\tau)$ is given by (7.8). A little analysis shows that in the tail of the echo, i.e. when $\tau > \sigma/2c$, $\epsilon(\tau)$ takes the constant value

$$\epsilon(\tau) \xrightarrow{\tau>\sigma/2c} 0.435, \tag{7.30}$$

which is the smallest possible value of $\epsilon(\tau)$, corresponding to the narrowest possible distribution $\mathscr{E}(q,\tau)$, which occurs (7.24a) when $E(k,\tau)$ is an annular delta-function of $K \equiv |\boldsymbol{K}|$. In the head of the echo, $\epsilon(\tau)$ increases a little as τ decreases – i.e. the fading becomes more irregular – until, at $\tau = 0$, ϵ has the value

$$\epsilon(0) = 0.562. \tag{7.31}$$

Thus there is a spread in fading wavelengths for the echo wavefunction, even for long delay times; this is due to the assumed azimuthal isotropy of the source – if the emitted pulse were confined to a narrow fan in the vertical plane containing the direction of motion of the source, it would be possible for $\mathscr{E}(q,\tau)$ to be arbitrarily sharp, and $\epsilon(\tau)$ could tend to zero for large τ, i.e. the spatial fading could be precisely periodic. We are not asserting that the considerable wavelength differences (7.30) or (7.31) will be encountered in *successive* intervals between zeros, because we have not examined the degree of correlation between neighbouring intervals.

To conclude this section, we examine the form of the autocorrelation $C_\psi(\tau,R)$ as given by the equations (5.28) and (5.30), and, in particular, we ask for the separation $R_{\max}(\tau)$ in source-receiver positions beyond which the echoes are no longer correlated. The integrands of the expressions for $C_\psi(\tau,R)$ contain an oscillatory factor (the Bessel function), while the other factors constitute a positive peak centred on $\tau' = \tau$ with width σ/c. If R is so large that more than one complete oscillation of the J_0-factor is contained within this peak, the value of the integral will be very small; thus we obtain

$$R_{\max}(\tau) \approx \frac{\lambda}{\sigma}(ch\tau)^{\frac{1}{2}}, \tag{7.32}$$

which is valid in the echo tail, where $\tau > \sigma/2c$. There is a simple physical interpretation of this result: if the finite width of the annulus in figure 7 is taken into account, it is clear that in order for any correlation in the spatial fading to occur, the change in the path difference $P_1M - P_2M$ as M moves across the annulus must not exceed about $\frac{1}{2}\lambda$ and this occurs when $|\Delta\boldsymbol{R}_0| = R_{\max}(\tau)$ as given by (7.32). (It is generally the case that $R_{\max}(\tau) < \Delta R(\tau)$, so that the correlations vanish before (5.19) is violated.)

Between points which are correlated, i.e. when $R \ll R_{\max}(\tau)$, the J_0-factor in the expressions for $C_\psi(\tau,R)$ varies slowly and the integrals are dominated by the peak at $\tau' = \tau$; thus

$$C_\psi(\tau,R) \overset{R\ll R_{\max}(\tau)}{\approx} J_0(2R\omega_0\sqrt{(\tau/ch)}). \tag{7.33}$$

The correlations in the tail of the echo (where $R_{\max}(\tau)$ is large) are therefore oscillatory out to $R = R_{\max}(\tau)$, while in the head of the echo (i.e. for $\tau < \sigma/2c$) we expect that $C_\psi(\tau,R)$ will have fallen to zero before $J_0(2R\omega_0(\tau/ch)^{\frac{1}{2}})$ begins to oscillate.

To illustrate these properties of the autocorrelation function, figure 8 shows $C_\psi(\tau,R)$ against R, computed for four different delay times τ; it is clear that as τ decreases, $C_\psi(\tau,R)$ departs increasingly from the limiting form (7.33), as we would expect.

Finally, we evaluate $C_\psi(\tau,R)$ in the *monochromatic limit* $\sigma/\lambda \to \infty$; then τ is always within the main body of the echo, there being no tail. The pulse envelope $a(t)$ is constant, and (5.28) and (5.30), together with (6.8 to 10), yield

$$C_\psi(\tau,R) \xrightarrow{\sigma/\lambda\to\infty} C_f\left(\frac{2S\omega_0 R}{c}\Big/\sqrt{(1-\exp\{-4S^2\omega_0^2/c^2\})}\right) \quad \text{surface } \alpha, \tag{7.34}$$

$$\longrightarrow C_f(R) \quad \text{surface } \beta, \tag{7.35}$$

$$\longrightarrow C_Z(R) \quad \text{surface } \gamma. \tag{7.36}$$

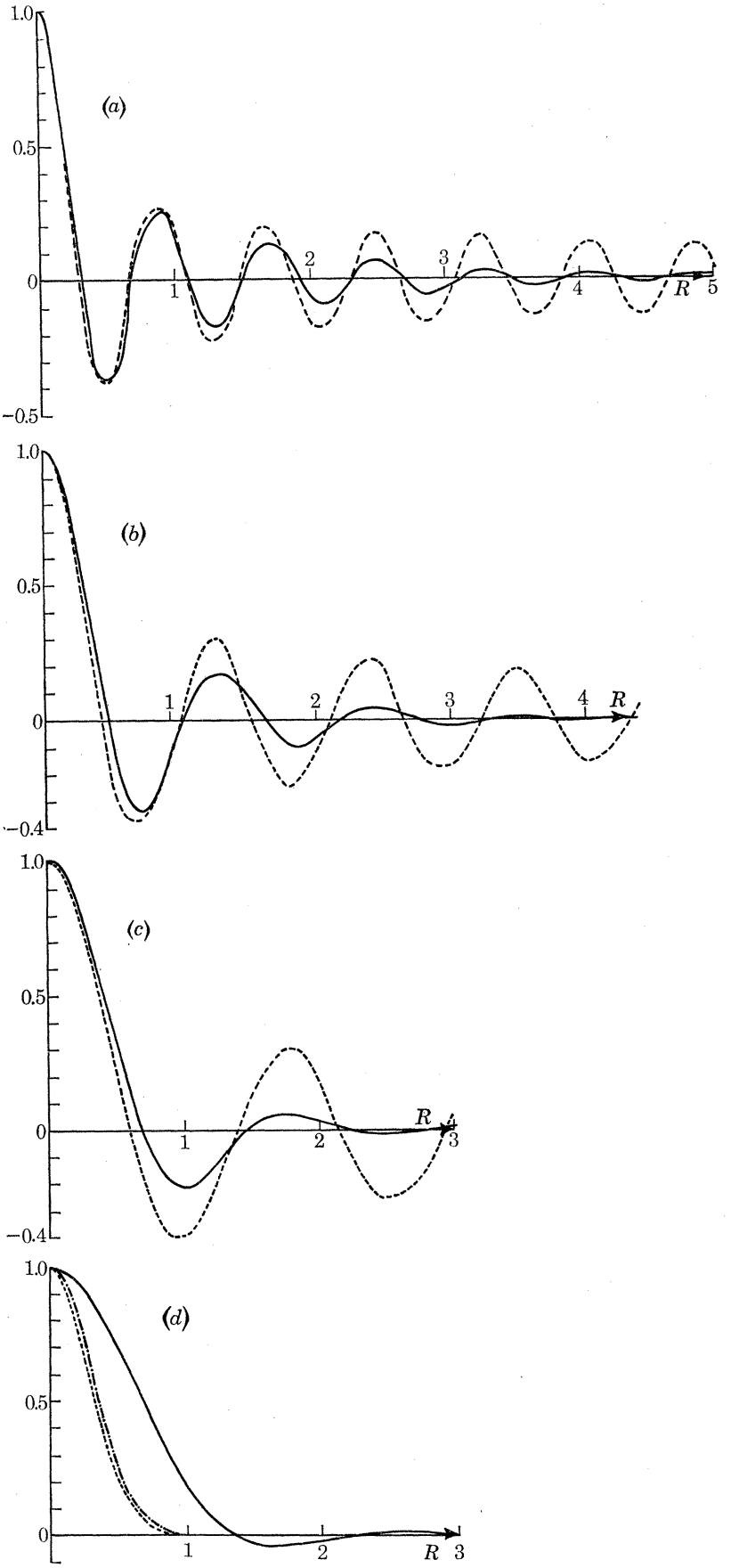

FIGURE 8. Echo spatial autocorrelation function for four different delay times ($\lambda = 1$, $h = 100$, $S = 1$, $L = 5$, undulating rough surface α). (*a*) $\sigma = 10$, $c\tau = 40$; ———, $C(\tau, R)$; – – – –, $J_0\{(4\pi R/\lambda)\,(c\tau/h)^{\frac{1}{2}}\}$; $R_{\max} = 6.3$. (*b*) $\sigma = 10$, $c\tau = 20$; ———, $C(\tau, R)$; – – – –, $J_0\{(4\pi R/\lambda)\,(c\tau/h)^{\frac{1}{2}}\}$; $R_{\max} = 4.5$ (*c*) $\sigma = 10$, $c\tau = 10$; ———, $C(\tau, R)$; – – – –, $J_0\{(4\pi R/\lambda)\,(c\tau/h)^{\frac{1}{2}}\}$; $R_{\max} = 3.16$. (*d*) $c\tau = 0$; ———, $C(\tau, R)$ for $\sigma = 10$; –·–·–, $C(\tau, R)$ for $\sigma = 100$; – – – –, $C(\tau, R)$ in monochromatic limit $\sigma \to \infty$ (7.34).

These expressions are independent of h, which is consistent with the proof by Booker *et al.* (1950) that the echo wavefunction 'conserves' its autocorrelation function as the source is raised above the reference plane, when the wave is monochromatic. We can check the results, (7.34) to (7.36), by examining the case when h is very small; the diffraction integral (2.12) gives, if $F(t)$ is monochromatic

$$\psi_c(\tau, \boldsymbol{R}_0) \xrightarrow{h\to 0} -\frac{\exp\{-i\omega_0\tau\}}{2h} Z(\boldsymbol{R}_0) \exp\{-2if(\boldsymbol{R}_0)\,\omega_0/c\}. \tag{7.37}$$

The autocorrelation function of this wavefunction equals (7.35) and (7.36) precisely for the surfaces β and γ, while for the undulating surface α, (7.37) gives

$$C_\psi(\tau, R) \xrightarrow{\sigma\to\infty} \frac{\exp\{4S^2\omega_0^2 C_f(R)/c^2\} - 1}{\exp\{4S^2\omega_0^2/c^2\} - 1}, \tag{7.38}$$

a formula equivalent to (7.34) for large and small R when S is large or moderate, and for all R when S is small, as would be expected in view of the basic substitution (3.23). The approach to the monochromatic limit is illustrated by figure 8*d*, which shows $C_\psi(\tau = 0, R)$ for pulses of three different lengths.

All of these properties of the autocorrelation function of the echo wavefunction have their counterparts for the autocorrelation functions of the smoothed power, and of the amplitude, since these quantities are given by (4.23) and (4.29) respectively.

7 (ii). *Ultimate sensitivity of position location by the use of echo fading*

In this section we deal with the use of the spatial fading of the echo to detect a horizontal movement $\Delta\boldsymbol{R}_0$ of the source-receiver relative to the rough surface. It is sensible to employ the smoothed power, or the amplitude ρ, rather than the wavefunction itself, because $\psi(\tau, \boldsymbol{R}_0)$ is phase-sensitive to h, and the result of an accidental change in height might be misinterpreted as spatial fading (a method for using this phase information for precise measurement of changes in h is suggested by Nye *et al.* 1972*b*). We ask: what is the smallest value of $|\Delta\boldsymbol{R}_0|$ which can be detected by observing the fading of ρ?

The answer involves the spatial rate of change of ρ, whose r.m.s. value at time delay τ, $\langle\rho'^2\rangle_\tau^{\frac{1}{2}}$, is given by (4.35). Precisely the same methods as were used in §7 (i) to calculate the fading frequency $N_\xi(\tau)$ can be used for $\langle\rho'^2\rangle_\tau^{\frac{1}{2}}$, with the result

$$\langle\rho'^2\rangle_\tau^{\frac{1}{2}} = \frac{4\pi}{\lambda}\left(\frac{c\bar{\tau}(\tau)\,\Sigma(\tau)}{2h}\right)^{\frac{1}{2}}, \tag{7.39}$$

where $\bar{\tau}(\tau)$ is given by (7.8) and figure 6, while $\Sigma(\tau)$ is given by (5.27) or (5.29). Let us denote by $\Delta\rho$ the smallest change in echo amplitude which can be detected above instrumental noise, and assume that by judicious siting of the apparatus a place can be found where ρ is varying n times as fast as its r.m.s. value. Then (7.39) gives, for the minimum detectable displacement at time delay τ,

$$|\Delta\boldsymbol{R}_0|_{\min,\tau} = \frac{\lambda\Delta\rho}{4\pi n}\left(\frac{2h}{c\bar{\tau}(\tau)\,\Sigma(\tau)}\right)^{\frac{1}{2}}. \tag{7.40}$$

This quantity is large for small τ, because the fading wavelength is large near the first return, and it is large for large τ, because although the fading wavelength is smallest in the tail, the mean echo power Σ is very small, and the signal is lost in the noise. Thus there is an optimum time delay, at which the echo is most sensitive to changes in position; this is $\tau_{\min}$, given by

$$\frac{\mathrm{d}}{\mathrm{d}\tau}[\bar{\tau}(\tau)\,\Sigma(\tau)]^{\frac{1}{2}}_{\tau=\tau_{\min}} = 0. \tag{7.41}$$

To estimate this quantity we assume that the echo has an appreciable tail, so that the half-length T discussed in § 6 (iii) exceeds about σ. The limiting forms of $\Sigma(\tau)$ (§ 6 (ii)) and $\bar{\tau}(\tau)$ (7.10) then yield

$$\tau_{\min} \approx \tfrac{4}{3}T, \tag{7.42}$$

where T is given by (6.14) and (6.15) (it should not be forgotten that T is measured from the origin of τ).

Thus, when the echo amplitude is most sensitive to horizontal movement, the smallest detectable displacement is

$$|\Delta \boldsymbol{R}_0|_{\min} \approx \frac{0.2\lambda}{n}\left(\frac{h}{cT}\right)^{\frac{1}{2}} \frac{\Delta\rho}{[\langle\rho^2\rangle_{4T/3}]^{\frac{1}{2}}}. \tag{7.43}$$

For the undulating surface α, which is surely the surface most likely to be found in nature, this result takes on a very convenient form; using (6.14) and the surface slope distribution (3.22), we get

$$|\Delta \boldsymbol{R}_0|_{\min} \approx \frac{0.2\lambda}{n[\langle f'^2\rangle]^{\frac{1}{2}}} \frac{\Delta\rho}{[\langle\rho^2\rangle_{4T/3}]^{\frac{1}{2}}}. \tag{7.44}$$

As an example, suppose that $n = 2$, that the r.m.s. surface slope is 10°, and that the instrument can detect a change in ρ of about 2 % of the r.m.s. amplitude when $\tau \approx T$; then a change in position of about 1 % of a wavelength could be detected. Accuracy of this order has already been achieved in Antarctic radar echo research by Walford (1972).

8. Summary of principal results: conclusions

We have calculated a number of statistical properties of the echo returned from the three rough surfaces introduced in § 3. In this section we reproduce the principal formulae, employing the original equation numbers to facilitate reference to the derivations.

Half the echo power arrives over a time $T+\frac{1}{2}\sigma$ (§ 6 (iii)) which is generally long compared with the duration σ/c of the pulse sent out from the source. The 'half-power' time T (measured from $\tau = 0$) is given by

$$T = 2.77hS^2/cL^2 \quad \text{(surface } \alpha\text{)}, \tag{6.14}$$

$$T = \frac{3h\lambda^2}{16\pi^2 cL^2}(1-\delta) \quad \text{(surfaces } \beta, \gamma\text{)}. \tag{6.15}$$

The form of the tail of late returns of the echo power is given by

$$\langle\psi^2(\tau, \boldsymbol{R}_0)\rangle \xrightarrow{\tau \gg \sigma/2c} \text{const.} \times Q(\tau), \tag{6.6), (6.7}$$

where $Q(\tau)$ is defined by (5.35) and (5.36). Whenever a tail is observed, broadening the echo power significantly, the reflexion is incoherent, as discussed in § 6 (ii); then only $\Sigma(\tau)$, the variance of the echo $\psi(\tau, \boldsymbol{R}_0)$, contributes to the echo power (6.1), the average echo wavefunction $\langle\psi(\tau, \boldsymbol{R}_0)\rangle$ being negligible (§ 5 (i)).

When the r.m.s. surface height S does not exceed the pulse-length σ, the general formula for the average echo power, showing the transition from coherence ($\delta = 1$) to incoherence ($\delta = 0$), is

$$\langle\psi^2(\tau, \boldsymbol{R}_0)\rangle \overset{\sigma > S}{=} \frac{\langle Z^2\rangle}{8h^2}\left\{2\delta a^2(\tau)\cos^2\omega_0\tau + (1-\delta)\int_0^\infty \mathrm{d}\tau' Q(\tau')\, a^2(\tau-\tau')\right\}, \tag{5.37}$$

where we have also used (6.1) and (5.6).

These properties of $\langle\psi^2(\tau, \boldsymbol{R}_0)$ suggest a method for inferring the nature of the surface from observations on the echo, outlined in §6 (ix).

The 'spatial fading' of the echo as the source-receiver position $\boldsymbol{R}_0$ is varied is not a potential source of extra information about the form of the rough surface. As shown in §7, this fading is a consequence of the Gaussian noise properties of the echo, together with the quasi-monochromaticity of the original pulse. A convenient statistical parameter describing the fading of the time-smoothed echo power introduced in §2 (ii) is $N_\rho^{\max}(\tau)$, the average number of times that the echo amplitude ρ (4.3) passes through the value $\Sigma^{\frac{1}{2}}$ when the source-receiver is moved through unit distance along a horizontal straight line, $\Sigma^{\frac{1}{2}}$ being the amplitude level where the fading is fastest. We found that

$$N_\rho^{\max}(\tau) = \frac{4.24}{\lambda}\left(\frac{c\bar{\tau}(\tau)}{h}\right)^{\frac{1}{2}} \frac{(1+(c\bar{\tau}(\tau)/4h))^{\frac{1}{2}}}{1+(c\bar{\tau}(\tau)/2h)} \qquad (7.4), (7.17)$$

where, to a close approximation, $$\bar{\tau}(\tau) = \frac{\int_0^\infty \mathrm{d}\tau' \tau' a^2(\tau-\tau')}{\int_0^\infty \mathrm{d}\tau' a^2(\tau-\tau')}, \qquad (7.8)$$

a function plotted in figure 6.

It is possible, however, to employ the spatial fading as a very sensitive indicator of horizontal movement of the source-receiver relative to the rough surface, the smallest detectable displacement being

$$|\Delta \boldsymbol{R}_0|_{\min} \approx \frac{0.2\lambda}{n}\left(\frac{h}{cT}\right)^{\frac{1}{2}} \frac{\Delta\rho}{[\langle\rho^2\rangle_{4T/3}]^{\frac{1}{2}}}. \qquad (7.43)$$

The portion of the echo just after the half-power time is most sensitive to horizontal displacements.

The theory of this paper could be extended in at least three directions. First, the restriction to statistically isotropic rough surfaces could be removed; this would be necessary in treating reflexion from, say, a surface of randomly spaced ridges, and would result in an echo autocorrelation function $C_\psi(\tau, \boldsymbol{R})$ which depends on the direction as well as the magnitude of the separation $\boldsymbol{R}$ between two source-receiver positions.

Secondly, the statistics of the echo as a function of time delay τ could be investigated; we have simply calculated the *average* echo wavefunction and power at time delay τ, and confined our discussion of fading – i.e. of departures from the average values – to variations in $\boldsymbol{R}_0$ at fixed τ. A theory of the statistics of $\psi(\tau, \boldsymbol{R}_0)$ in the three-dimensional 'space' specified by τ and $\boldsymbol{R}_0$ is necessary in order to understand the statistical topology of the surfaces on which $\psi(\tau, \boldsymbol{R}_0)$ or $(\psi^2(\tau, \boldsymbol{R}_0))_{\mathrm{sm}}$ is constant. For example, it would be desirable to predict the average density of the 'dislocation lines' discovered by J. F. Nye (unpublished), which mark the places where zeros in the curve of $\psi(\tau, \boldsymbol{R}_0)$ against τ appear or disappear as $\boldsymbol{R}_0$ varies. The problem is a difficult one, because the statistics of the echo are non-stationary in τ, due to the τ-dependence of $\langle\psi(\tau, \boldsymbol{R}_0)\rangle$ (§5 (i)) and $\langle\psi^2(\tau, \boldsymbol{R}_0)\rangle$ (§6).

Finally, the 'partial ensemble averaging' over 'neighbourhoods' which must be employed (§1) when there is a continuous transition between 'roughness' and 'geography' should be put on a more secure mathematical foundation. Again the difficulty arises because the echo statistics are non-stationary, this time in the variable $\boldsymbol{R}_0$.

It is a pleasure to thank Professor J. F. Nye for his constant encouragement and keen criticisms, which led to a complete rewriting of the paper, and Drs M. E. R. Walford and D. A. Greenwood for many helpful discussions and suggestions.

PHILOSOPHICAL TRANSACTIONS OF THE ROYAL SOCIETY A MATHEMATICAL, PHYSICAL & ENGINEERING SCIENCES

Appendix 1

It is required to derive (4.34) from (4.33), and (4.38) from (4.37), using (4.24) and (4.5). First we evaluate $P_2^{\rho}(\rho_1, \rho_2, \mathrm{d}\boldsymbol{R})$ where $|\mathrm{d}\boldsymbol{R}|$ is small. We can replace $C_{\psi_c\psi_c^*}(\mathrm{d}\boldsymbol{R})$ by

$$C_{\psi_c\psi_c^*}(\mathrm{d}\boldsymbol{R}) \approx 1 - \tfrac{1}{2}|\mathrm{d}\boldsymbol{R}|^2 |C''_{\psi_c\psi_c^*}(0)|, \tag{A 1}$$

so that (4.24) gives, on using (4.5)

$$P_2^{\rho}(\rho_1, \rho_2, \mathrm{d}\boldsymbol{R}) = \frac{\rho_1\rho_2}{4\pi\Sigma^2|\mathrm{d}\boldsymbol{R}|^2 C''} \int_0^{2\pi} \mathrm{d}\chi_1 \int_0^{2\pi} \mathrm{d}\chi_2 \exp\left\{-\frac{(\rho_1^2+\rho_2^2-2\rho_1\rho_2\cos(\chi_1-\chi_2))}{2\Sigma|\mathrm{d}\boldsymbol{R}|^2 C''}\right\}$$
$$\times \exp\left\{-\frac{\begin{array}{r}(\rho_1\rho_2\cos(\chi_1-\chi_2)+\langle\xi\rangle^2+\langle\eta\rangle^2-\rho_1\cos\chi_1\langle\xi\rangle \\ -\rho_2\cos\chi_2\langle\xi\rangle-\rho_1\sin\chi_1\langle\eta\rangle-\rho_2\sin\chi_2\langle\eta\rangle)\end{array}}{2\Sigma}\right\}, \tag{A 2}$$

where we have retained terms up to zero order in $|\mathrm{d}\boldsymbol{R}|$ in the exponent, and used the abbreviation

$$C'' \equiv |C''_{\psi_c\psi_c^*}(0)|. \tag{A 3}$$

Because of the appearance of $|\mathrm{d}\boldsymbol{R}|^2$ in the denominator of the first exponent in (A 2), the first exponential factor is very sharply peaked about $\chi_1 = \chi_2$, and the method of steepest descent may be used to evaluate the integral over χ_2, to lowest order in $|\mathrm{d}\boldsymbol{R}|$. This gives

$$P_2^{\rho}(\rho_1, \rho_2, \mathrm{d}\boldsymbol{R}) = \left(\frac{\rho_1\rho_2}{2\pi C''\Sigma}\right)^{\frac{1}{2}} \frac{\exp\{-(\rho_1-\rho_2)^2/2\Sigma C''|\mathrm{d}\boldsymbol{R}|^{\frac{1}{2}}\}}{2\pi\Sigma|\mathrm{d}\boldsymbol{R}|}$$
$$\times \int_0^{2\pi} \mathrm{d}\chi_1 \exp\left\{\frac{-\rho_1\rho_2-\langle\xi\rangle^2-\langle\eta\rangle^2+(\rho_1+\rho_2)(\cos\chi_1\langle\xi\rangle+\sin\chi_1\langle\eta\rangle)}{2\Sigma}\right\} \tag{A 4}$$

$$= \left(\frac{\rho_1\rho_2}{2\pi C''\Sigma}\right)^{\frac{1}{2}} \frac{\exp\left\{-\left\{\frac{(\rho_1-\rho_2)^2}{2\Sigma C''|\mathrm{d}\boldsymbol{R}|^2}+\frac{(\rho_1\rho_2+\langle\xi\rangle^2+\langle\eta\rangle^2)}{2\Sigma}\right\}\right\}}{\Sigma|\mathrm{d}\boldsymbol{R}|} I_0\left(\frac{\rho_1+\rho_2}{2\Sigma}(\langle\xi\rangle^2+\langle\eta\rangle^2)^{\frac{1}{2}}\right). \tag{A 5}$$

On setting $\rho_1 = \rho$, $\rho_2 = \rho + \rho'|\mathrm{d}\boldsymbol{R}|$ and noting (4.25), (4.34) follows at once.

In order to perform the double integration in (4.37), it is only necessary to realize that (A 5) is negligible unless $\rho_1 \approx \rho_2$, which, together with the limits in (4.37), implies that we can set $\rho_1 \approx \rho_2 \approx \rho_D$ everywhere in (A 5) except the first exponential factor. Then we use the formula

$$\lim_{(|\mathrm{d}R|\to 0)} \int_0^{\rho_D} \mathrm{d}\rho_1 \int_{\rho_D}^{\infty} \mathrm{d}\rho_2 \exp\{-(\rho_1-\rho_2)^2/2\Sigma C''|\mathrm{d}\boldsymbol{R}|^2\} = \Sigma C''|\mathrm{d}\boldsymbol{R}|^2, \tag{A 6}$$

and (4.38) follows immediately.

Appendix 2

The step from (5.12) to (5.13) requires the proof of the relation

$$I \equiv \iint \mathrm{d}\boldsymbol{R}_1 \iint \mathrm{d}\boldsymbol{R}_2 \exp\left\{\frac{\mathrm{i}}{hc}(\omega_1 R_1^2 - \omega_2|\boldsymbol{R}_2-\boldsymbol{R}|^2)\right\} \bar{P}_2\left(\frac{2\omega_2}{c}, \frac{2\omega_1}{c}, |\boldsymbol{R}_2-\boldsymbol{R}_1|\right)$$
$$= 2\pi^2 ch \int_0^{\infty} \mathrm{d}\tau' \exp\{\mathrm{i}(\omega_1-\omega_2)\tau'\} J_0\left(2R\left(\frac{\omega_1\omega_2\tau'}{ch}\right)^{\frac{1}{2}}\right)$$
$$\times \int_0^{\infty} \mathrm{d}R' R' J_0\left(2R'\left(\frac{\omega_1\omega_2\tau'}{ch}\right)^{\frac{1}{2}}\right) \bar{P}_2\left(\frac{2\omega_2}{c}, \frac{2\omega_1}{c}, R'\right), \tag{A 7}$$

where ω_1 and ω_2 are positive. To evaluate the integrals over $\boldsymbol{R}_1$ and $\boldsymbol{R}_2$ we change variables to $\boldsymbol{R}_2$ and $\boldsymbol{R}' \equiv \boldsymbol{R}_2 - \boldsymbol{R}_1$, which we express in polar coordinates; this gives

$$I = \int_0^{\infty} \mathrm{d}R_2 R_2 \int_0^{2\pi} \mathrm{d}\theta_2 \int_0^{\infty} \mathrm{d}R' R' \int_0^{2\pi} \mathrm{d}\theta' \exp\left\{\frac{\mathrm{i}}{hc}[\omega_1(R_2^2+R'^2+2R_2R'\cos\theta')\right.$$
$$\left. -\omega_2(R_2^2+R^2-2R_2R\cos\theta_2)]\right\} \bar{P}_2\left(\frac{2\omega_2}{c}, \frac{2\omega_1}{c}, R'\right). \tag{A 8}$$

where we have measured θ' from the direction $\boldsymbol{R}_2$, and θ_2 from the direction $\boldsymbol{R}$. The angular integrations define Bessel functions (Gradshteyn & Ryzhik 1965, equation 8.411.1), so that

$$I = 4\pi^2 \int_0^\infty \mathrm{d}R_2 \int_0^\infty \mathrm{d}R' R_2 R' \exp\left\{\frac{\mathrm{i}}{hc}\left[(\omega_1-\omega_2)\, R_2^2 + \omega_1 R'^2 - \omega_2 R^2\right]\right\} \times J_0\left(\frac{2R_2 R'\omega_1}{hc}\right) J_0\left(\frac{2R_2 R\omega_2}{hc}\right) \bar{P}_2\left(\frac{2\omega_2}{c}, \frac{2\omega_1}{c}, R'\right). \quad \text{(A 9)}$$

The integral over R_2 is equation 6.633.2 of Gradshteyn & Ryzhik (1965), which gives

$$I = \frac{2\pi^2 \mathrm{i} hc}{\omega_1-\omega_2} \int_0^\infty \mathrm{d}R' R' \exp\left\{-\frac{\mathrm{i}\omega_1\omega_2(R'^2+R^2)}{hc(\omega_1-\omega_2)}\right\} J_0\left(\frac{2R'R\omega_1\omega_2}{hc(\omega_1-\omega_2)}\right) \bar{P}_2\left(\frac{2\omega_2}{c}, \frac{2\omega_1}{c}, R'\right). \quad \text{(A 10)}$$

Now we introduce the dummy delay time variable τ'; by writing

$$I = 2\pi^2 ch \int_0^\infty \mathrm{d}R' R' \int_{-\infty}^\infty \mathrm{d}\tau' \exp\{\mathrm{i}(\omega_1-\omega_2)\,\tau'\}\, M(\tau')\, \bar{P}_2\left(\frac{2\omega_2}{c}, \frac{2\omega_1}{c}, R'\right), \quad \text{(A 11)}$$

so that $M(\tau')$ is defined by

$$M(\tau') \equiv \frac{\mathrm{i}}{2\pi} \int_{-\infty}^\infty \frac{\mathrm{d}\Omega \exp\{-\mathrm{i}\Omega\tau'\}}{\Omega} \exp\left\{-\frac{\mathrm{i}\omega_1\omega_2(R'^2+R^2)}{ch\Omega}\right\} J_0\left(\frac{2RR'\omega_1\omega_2}{ch\Omega}\right). \quad \text{(A 12)}$$

The essential singularities of the integrand at $\Omega = 0$ and $\Omega = \infty$ imply that

$$M(\tau') = 0 \quad \text{if} \quad \tau' < 0. \quad \text{(A 13)}$$

For $\tau' > 0$, a straightforward change of variable gives

$$M(\tau') = \frac{1}{2\pi\mathrm{i}} \int_{-\mathrm{i}\infty+\epsilon}^{\mathrm{i}\infty+\epsilon} \frac{\mathrm{d}y}{y} \exp\left\{\frac{1}{2}\left(y - \frac{4\omega_1\omega_2(R^2+R'^2)\,\tau'}{chy}\right)\right\} I_0\left(\frac{4RR'\omega_1\omega_2\tau'}{chy}\right), \quad \text{(A 14)}$$

which is a standard integral (Gradshteyn & Ryzhik 1965, equation 8.4.24) with the value

$$M(\tau') = J_0\left(2R\left(\frac{\omega_1\omega_2\tau'}{ch}\right)^{\frac{1}{2}}\right) J_0\left(2R'\left(\frac{\omega_1\omega_2\tau'}{ch}\right)^{\frac{1}{2}}\right). \quad \text{(A 15)}$$

This result, together with (A 13) and (A 11), gives (A 7) immediately. This method seems rather long-winded, but I cannot find a simpler one.

References

Beckmann, P. & Spizzichino, A. 1963 *The scattering of electromagnetic waves from rough surfaces*. Oxford and New York: Pergamon.

Berry, M. V. 1972 *J. Phys.* A **5**, 272–291.

Booker, H. G., Ratcliffe, J. A. & Shinn, D. H. 1950 *Phil. Trans. Roy. Soc. Lond.* A **242**, 579–607.

Gradshteyn, I. S. & Ryzhik, I. M. 1965 *Tables of integrals, series, and products*. New York and London: Academic Press.

Harrison, C. H. 1970 *Geophysics* **35**, 1099–1115.

Harrison, C. H. 1972 Radio propagation effects in glaciers. Ph.D. Thesis, Cambridge, U.K.

Longuet-Higgins, M. S. 1956 *Phil. Trans. R. Soc. Lond.* A **249**, 321–387.

Mercier, R. P. 1962 *Proc. Camb. Phil. Soc.* **58**, 382–400.

Nye, J. F. 1970 *Proc. R. Soc. Lond.* A **315**, 381–403.

Nye, J. F., Kyte, R. G. & Threlfall, D. C. 1972*a* *J. Glaciol.* **63**, 319–325.

Nye, J. F., Berry, M. V. & Walford, M. E. R. 1972*b* *Nature, Lond.* **240**, 7–9.

Rice, S. O. 1944 *Bell Syst. tech. J.* **23**, 282–332.

Rice, S. O. 1945 *Bell Syst. tech. J.* **24**, 46–156.

Robin, G. de Q., Evans, S. & Bailey, J. T. 1969 *Phil. Trans. R. Soc. Lond.* A **265**, 437–505.

Walford, M. E. R. 1972 *Nature, Lond.* **239**, 93–95.